2022

Photorespiration in Eelgrass (*Zostera marina* L.): A Photoprotection Mechanism for Survival in a CO_2-Limited World

Billur Celebi-Ergin
celebibillur@gmail.com

Richard C. Zimmerman
Old Dominion University, rzimmerm@odu.edu

Victoria J. Hill
Old Dominion University, vhill@odu.edu

Original Publication Citation

Celebi-Ergin B., Zimmerman R.C. and Hill V.J. (2022) Photorespiration in eelgrass (*Zostera marina* L.): A photoprotection mechanism for survival in a CO_2-limited world. *Frontiers in Plant Science, 13*, 1-19, Article 1025416. https://doi.org/10.3389/fpls.2022.1025416

frontiers | Frontiers in Plant Science

TYPE Original Research
PUBLISHED 11 November 2022
DOI 10.3389/fpls.2022.1025416

OPEN ACCESS

EDITED BY
Benoit Schoefs,
Le Mans Université, France

REVIEWED BY
Milan Szabo,
Eötvös Loránd Research Network (ELKH), Hungary
Alexandrina Stirbet,
University of Bucharest, Romania

*CORRESPONDENCE
Billur Celebi-Ergin
celebibillur@gmail.com

†PRESENT ADDRESS
Billur Celebi-Ergin,
Department of Molecular Biology and Genetics, Koç University Rumelifeneri Yolu Sariyer, Istanbul, Turkey

SPECIALTY SECTION
This article was submitted to Marine and Freshwater Plants, a section of the journal Frontiers in Plant Science

RECEIVED 22 August 2022
ACCEPTED 10 October 2022
PUBLISHED 11 November 2022

CITATION
Celebi-Ergin B, Zimmerman RC and Hill VJ (2022) Photorespiration in eelgrass (*Zostera marina* L.): A photoprotection mechanism for survival in a CO_2-limited world. *Front. Plant Sci.* 13:1025416. doi: 10.3389/fpls.2022.1025416

Photorespiration in eelgrass (*Zostera marina* L.): A photoprotection mechanism for survival in a CO_2-limited world

Billur Celebi-Ergin *†, Richard C. Zimmerman and Victoria J. Hill

Department of Ocean and Earth Sciences, Old Dominion University, Norfolk, VA, United States

Photorespiration, commonly viewed as a loss in photosynthetic productivity of C3 plants, is expected to decline with increasing atmospheric CO_2, even though photorespiration plays an important role in the oxidative stress responses. This study aimed to quantify the role of photorespiration and alternative photoprotection mechanisms in *Zostera marina* L. (eelgrass), a carbon-limited marine C3 plant, in response to ocean acidification. Plants were grown in controlled outdoor aquaria at different $[CO_2]_{aq}$ ranging from ~55 (ambient) to ~2121 μM for 13 months and compared for differences in leaf photochemistry by simultaneous measurements of O_2 flux and variable fluorescence. At ambient $[CO_2]$, photosynthesis was carbon limited and the excess photon absorption was diverted both to photorespiration and non-photochemical quenching (NPQ). The dynamic range of NPQ regulation in ambient grown plants, in response to instantaneous changes in $[CO_2]_{aq}$, suggested considerable tolerance for fluctuating environmental conditions. However, 60 to 80% of maximum photosynthetic capacity of ambient plants was diverted to photorespiration resulting in limited carbon fixation. The photosynthesis to respiration ratio (P_E : R_D) of ambient grown plants increased 6-fold when measured under high CO_2 because photorespiration was virtually suppressed. Plants acclimated to high CO_2 maintained 4-fold higher P_E : R_D than ambient grown plants as a result of a 60% reduction in photorespiration. The O_2 production efficiency per unit chlorophyll was not affected by the CO_2 environment in which the plants were grown. Yet, CO_2 enrichment decreased the light level to initiate NPQ activity and downregulated the biomass specific pigment content by 50% and area specific pigment content by 30%. Thus, phenotypic acclimation to ocean carbonation in eelgrass, indicating the coupling between the regulation of photosynthetic structure and metabolic carbon demands, involved the downregulation of light harvesting by the photosynthetic apparatus, a reduction in the role of photorespiration and an increase in the role of NPQ in photoprotection. The quasi-mechanistic model developed in this study

permits integration of photosynthetic and morphological acclimation to ocean carbonation into seagrass productivity models, by adjusting the limits of the photosynthetic parameters based on substrate availability and physiological capacity.

KEYWORDS

CO_2, non-photochemical quenching, ocean acidification, photorespiration, photosynthesis, quantum yield, seagrass

Introduction

Photosynthesis and photorespiration are competing processes due to the bi-functionality of ribulose 1,5-biphosphate carboxylase/oxygenase (Rubisco) (Spreitzer and Salvucci, 2002). Since the oxygenation reaction of Rubisco decreases photosynthetic carbon gain, it has been viewed as an inefficient legacy of evolution that might be engineered out of terrestrial plants in a quest for increased productivity (Andrews and Lorimer, 1978; Somerville, 2001; Xin et al., 2015). Recent work, however, suggests that Rubisco's CO_2/O_2 specificity in different species may approach optimal acclimation to their gaseous environment in which the plants are grown (Tcherkez et al., 2006; Bathellier et al., 2018). More importantly, especially for carbon-limited seagrasses, photorespiration may serve as an important metabolic "clutch" to protect the photochemical pathway at high irradiance (Heber and Krause, 1980; Osmond, 1981; Osmond et al., 1997; Igamberdiev et al., 2001). When the Calvin Benson cycle is limited by the availability of CO_2, continuation of light reactions over-reduces the thylakoid electron transport chain and generates O_2 and reactive oxygen species (ROS) that potentiates oxidative stress (Voss et al., 2013). Photorespiration helps to balance the redox state and minimize the accumulation of ROS by dissipating the excess reducing equivalents (NADPH) as well as energy (ATP) (Foyer et al., 2009). By recycling the photorespired CO_2, photorespiration may also facilitate carbon assimilation in CO_2 limited environments, thereby minimizing photosynthetic inefficiencies resulting from C-limitation (Busch et al., 2013; Xin et al., 2015).

Photorespiration is often considered to be of minor importance in aquatic systems as a result of carbon concentrating mechanisms (CCMs) that facilitate the transport of HCO_3^- and its dehydration by algal pyrenoids that effectively deliver CO_2 to Rubisco (Frost-Christensen and Sand-Jensen, 1992; Madsen et al., 1993; Meyer et al., 2017). In today's oceanic water (pH ~8.2), 89% of the DIC is in form of HCO_3^- and only 0.5% exists as dissolved CO_2 (Zeebe, 2012). However, not all aquatic C_3 plants have similar efficiencies to use both forms of DIC for photosynthesis (Raven and Beardall, 2003; Raven et al., 2011; Raven and Beardall, 2014). Additionally, CO_2 acquisition by simple diffusion through the leaf surface is more difficult for submerged plants due to the 10,000-fold lower diffusion rates of gases in a liquid environment relative to air (Borum et al., 2006). Consequently, for aquatic C_3 plants such as seagrasses that do not use CCMs effectively, carbon limitation likely increases the photorespiratory function of Rubisco (Tolbert and Osmond, 1976; Touchette and Burkholder, 2000).

Seagrasses are flowering marine plants that evolved from terrestrial monocots in the middle Cretaceous (Larkum et al., 2006b) when higher atmospheric and oceanic CO_2 concentrations likely supported photosynthesis and minimized photorespiration (Kuypers et al., 1999; Zeebe, 2012). In colonizing the aquatic habitat, seagrass evolved adaptations to a submerged environment that produced important anatomical differences from their terrestrial ancestors (Zimmerman et al., 1997; Larkum et al., 2006a). Seagrass leaves have no stomatal openings as gas exchange occurs across both leaf surfaces by diffusion, which uncouples carbon uptake from water relations. Seagrasses also have a lacunal system with aerenchyma extending from the roots to the leaves that facilitates the transport of O_2 to the roots buried in permanently flooded anoxic sediments, and allows transport of CO_2 from the roots to leaves, providing an alternative carbon source (Madsen and Sand-Jensen, 1991). Like their terrestrial ancestors, however, seagrass chloroplasts lack pyrenoids that serve as an important CCM in most aquatic algae (Meyer et al., 2017) and seagrasses are typically less efficient in utilizing HCO_3^- than macroalgae (Beer et al., 1991). Although Rubisco activity in seagrasses is lower than the typical activities in freshwater emergent angiosperms and marine red algae, it is comparable to that observed in marine green and brown macroalgae (Beer et al., 1991). Simulations of nearshore seawater DIC distribution during the Cretaceous period have predicted that photosynthetic rates of seagrasses would have been similar to macroalgae (Beer and Koch, 1996). However, in today's oceans, seagrass photosynthesis is generally considered to be

carbon limited (Durako, 1993; Beer and Koch, 1996; Zimmerman et al., 1997; Invers et al., 2001).

Carbon limited photosynthesis also restricts seagrasses to shallow, high light environments, where low daytime CO_2:O_2 ratios in the water column may increase seagrass vulnerability to photorespiration (Buapet et al., 2013b). The photorespiratory pathway was confirmed in marine plants and macrophytes by showing that photosynthesis could be inhibited by increasing the O_2 concentration, resulting in higher concentrations of glycolate pathway intermediates (Hough, 1974; Black et al., 1976; Burris et al., 1976; Downton et al., 1976; Hough and Wetzel, 1977; Andrews and Abel, 1979). The decreasing O_2 evolution rates relative to electron transfer rates measured by PAM fluorometry at high irradiances in *Zostera marina* and *Halophila stipulacea* also suggested a role for photorespiration in these seagrass species (Beer et al., 1998). More recent studies demonstrated the influence of oxygen concentrations and temperature on photorespiration in seagrass that fluctuate in natural environment because of eutrophication, high community productivity and elevated ocean temperatures; and therefore, will play a role in predicting the health status of these plants in warmer climate scenarios (Buapet and Björk, 2016; Rasmusson et al., 2020). The plastochron interval, which defines leaf life span, leaf turnover and elongation rates, plays an important role in photoacclimation strategies that differ among species at the chloroplast, leaf and shoot levels (Schubert et al., 2018). However, we still do not understand how long-term acclimation to climate warming and ocean acidification/carbonation will affect photorespiration and photoprotection in seagrasses (Koch et al., 2013).

Several experiments simulating ocean acidification/carbonation impacts on time scales of hours to >1 year have quantified the positive impacts of CO_2 availability on carbon balance, growth, survival and reproductive output in seagrasses (Zimmerman, 2021). During the most recent of these studies, the down-regulation of pigment content with increasing CO_2 resembled the photoacclimation response to high light environment that pointed to the importance of metabolic acclimation regulating the redox state of the chloroplast in eelgrass (Zimmerman et al., 2017; Celebi-Ergin et al., 2021). Therefore, the objectives of this study were to estimate the importance of photorespiration in the marine angiosperm *Zostera marina* L. (eelgrass) under today's oceanic carbon concentrations and explore the potential acclimation response to prolonged ocean acidification/carbonation by 1) quantifying the photochemical rates under different light and CO_2 availability by using eelgrass grown in a high light low CO_2 environment, i.e., representing the baseline photosynthetic capacity under today's oceanic conditions; and 2) comparing the relative contribution of different photochemical pathways in eelgrass after 13 months of acclimation to different CO_2 environments superimposed open daily and seasonal patterns of solar radiation, temperature and salinity.

Materials and methods

Table 1 provides a complete list of all abbreviations, acronyms, and symbols along with their units used throughout this paper.

The experimental facility and sampling from pH treatments

Eelgrass shoots used in this study were grown in an outdoor aquatic climate research facility at the Virginia Aquarium and Marine Science Center, VA, USA. The experimental design and control of manipulations for this-long term project were detailed in Zimmerman et al. (2017). Briefly, eelgrass plants, harvested in May 2013 from a subtidal population growing in South Bay, a coastal lagoon on the Virginia portion of the DelMarVa Peninsula, USA, were transplanted into 20 fiberglass open top aquaria (3 m^3 each) plumbed with running seawater from Owl's Creek, VA and exposed to natural sunlight. Temperature, pH, salinity, and irradiance were monitored continuously in all aquaria. Beverage-grade CO_2 gas was used to enrich the experimental aquaria from June 2013 to October 2014 using a system of pH-controlled solenoid valves. pH treatment levels ranged from pH 6 ($[CO_{2(aq)}] \cong 2121\ \mu M$) to ambient (no CO_2 addition, pH $\cong$ 7.7, $[CO_{2(aq)}] \cong 55\ \mu M$), with 0.5 pH intervals between the treatments (4 aquaria at each pH). The experimental CO_2 manipulation produced consistently different levels of $[CO_{2(aq)}]$ and pH among the treatments day and night throughout the duration of the 13-month experiment. Plant performance was monitored monthly while environmental parameters, which varied daily and seasonally, were recorded at 10-minute intervals.

During July 2014, after 13 months of cultivation in the experimental aquaria, freshly collected 2nd youngest leaves from pH 6.1 (2121 μM $CO_{2(aq)}$), pH 6.9 (371 μM $CO_{2(aq)}$) and ambient pH 7.7 (55 μM $CO_{2(aq)}$) treatments were harvested for laboratory measurements of photochemistry under fully controlled incubation conditions. Hereafter, the three treatments will be referred to as $G_{pH}6$, $G_{pH}7$ and $G_{pH}8$, for simplicity. During these measurements, the daily seawater temperature in aquaria ranged from 25 to 28°C; allowing all the incubation measurements described here to be conducted at the optimal temperature of 25°C without inducing heat stress. The daily total surface irradiance ranged from 10 to 29 mol photons m^{-2} d^{-1}; corresponding to more than 6 h of photosynthetically saturating irradiance (>200 μmol photons m^{-2} s^{-1}) per day, under which conditions the leaves of all plants should have been acclimated to a high light environment (Cummings and Zimmerman, 2003).

Incubation measurements of leaf photochemistry

Photosynthesis and respiration rates were measured using polarographic O_2 electrodes in temperature controlled, water-jacketed glass metabolic incubation chambers (Rank Bros.,

TABLE 1 List of symbols, their definitions, and dimensions.

Symbol	Definition	Dimensions
Chl-*a*	Chlorophyll *a*	μg cm^{-2} or mg g^{-1} FW
Chl-*b*	Chlorophyll *b*	μg cm^{-2} or mg g^{-1} FW
TChl	Total Chlorophyll	μg cm^{-2} or mg g^{-1} FW
TCar	Total Carotenoid	μg cm^{-2} or mg g^{-1} FW
FW	Fresh Weight	mg
LA	Leaf Area	cm^2
$A_L(\lambda)$	Leaf absorptance	Dimensionless
$D(\lambda)$	Leaf absorbance	Dimensionless
$R(\lambda)$	Leaf reflectance	Dimensionless
$a_L^*(\lambda)$	Optical cross-section	m^2 g^{-1} Chl-*a*
λ	Wavelength	nm
PAR	Photosynthetically active radiation	μmol photons s^{-1} m^{-2}
PUR	Photosynthetically usable radiation	μmol photons s^{-1} m^{-2}
E	Incident irradiance	μmol photons s^{-1} m^{-2}
E_k	Photosynthesis-saturating irradiance	μmol photons s^{-1} m^{-2}
P_g	Gross photosynthesis	μmol O$_2$ s^{-1} m^{-2} or μmol O$_2$ hr^{-1} mg^{-1} TChl
P_{net}	Net photosynthesis	μmol O$_2$ hr^{-1} g^{-1} FW or μmol O$_2$ hr^{-1} mg^{-1} TChl
P_E	light-saturated rate of gross photosynthesis	μmol O$_2$ s^{-1} m^{-2} or μmol O$_2$ hr^{-1} g^{-1} FW or μmol O$_2$ hr^{-1} mg^{-1} TChl
P_T	True photosynthesis	
P_R	Photorespiration	μmol O$_2$ hr^{-1} mg^{-1} TChl
R_D	Dark respiration	μmol O$_2$ hr^{-1} g^{-1} FW
α	Photosynthetic efficiency at light-limited region of PE curve	μmol O$_2$ μmol^{-1} photons
Φ_{O2}	Quantum yield of oxygen evolution	μmol O$_2$ μmol^{-1} photons
F_m, $F_{m'}$	Maximum fluorescence from dark and light adapted leaf	Dimensionless
F_0, $F_{0'}$	Minimum fluorescence from dark and light adapted leaf	Dimensionless
F_v	Variable fluorescence	Dimensionless
Φ_{PSII}	Effective Quantum yield of fluorescence ($[F_{m'} - F']/F_{m'}$)	Dimensionless
ETR	Electron transport rate	μmol electrons s^{-1} m^{-2}
NPQ	Nonphotochemical quenching ($[F_m - F_{m'}]/F_{m'}$)	Dimensionless

Parenthetic notation (λ) denotes wavelength dependence of the variable.

Cambridge, UK). Variable fluorescence was measured simultaneously on each leaf using a Pulse Amplitude Modulated (PAM) fluorometer (Mini PAM, Walz, Germany). Incubation seawater pH (a proxy for dissolved inorganic carbon (DIC) concentration) was measured using an epoxy mini-electrode and pH meter (Cole-Parmer) calibrated with NBS buffers. The lid of the incubation chamber was modified to hold the pH electrode in the incubation water and the miniature fiberoptic probe of the PAM device in close proximity to the leaf surface. The chamber was continuously mixed by a magnetic stirrer which homogenized the incubation medium and provided turbulent flow to reduce boundary layer limitation of gas exchange across the leaf surface. Continuous analog signals from the three sensors were recorded digitally using custom software written with LabView (2009 edition, National Instruments). Voltage data were post processed into metabolic rates using MATLAB R2014 (The MathWorks Inc.). A Kodak slide projector fitted with a halogen (ELH) bulb provided photosynthetically active radiation (PAR). The intensity of PAR was adjusted with neutral density filters and calibrated daily with a QSL 2100 scalar radiometer (Biospherical Instruments Inc.).

Concentrations of $CO_{2(aq)}$ in the aquaria and metabolic incubation chambers were determined from measured values of pH, alkalinity, salinity and temperature using CO2SYS (Ver. 2.1; Lewis and Wallace 1998). Leaves, harvested from plants grown at pH/CO_2 treatments $G_{pH}6$ ($[CO_{2(aq)}]$ = 2121 μM), $G_{pH}7$ ($[CO_{2(aq)}]$ = 371 μM) and $G_{pH}8$ ($[CO_{2(aq)}]$ =55 μM), were used to measure the photosynthetic response at pH/$CO_{2(aq)}$ levels of 6 ($M_{pH}6$), 7 ($M_{pH}7$) and 8 ($M_{pH}8$). Seawater [DIC] and pH in the incubation chambers were adjusted by bubbling with a gas mixture of CO_2, O_2 and N_2 that maintained [O_2] at air saturation (~215 μM). Seawater temperature was maintained at 25°C by a circulating water bath. Leaves were cleaned of epiphytes by gently scraping with a razor blade and kept in the dark for 20 minutes before the incubation measurements. A

separate three cm long pieces of leaf tissue, cut approximately one cm above the meristem, was used during each ten min dark (i.e., dark respiration) and ten min light (i.e., net photosynthesis) measurement. The pigment content and optical properties of the leaf tissues (Table 1) were measured after each incubation as described by Celebi-Ergin et al. (2021).

The seawater used during all incubations was collected in April 2014 from Owl's Creek, the tidal estuary used as source water for the experimental facility (Zimmerman et al., 2017). This seawater stock, with salinity of 24 (PSS-78, (Lewis, 1980) was filtered through 0.2 μm Nucleopore membrane filters and stored under refrigeration in dark bottles until used in these experiments. After incubations, alkalinity was determined on aliquots of seawater taken from the chamber using an automated potentiometric titrator (Metrohm). Table 2 summarizes measured parameters of seawater used in metabolic incubation chamber.

Determination of photochemical rates

Oxygen evolution rates of each tissue were separately normalized to fresh weight, leaf area and total pigment concentration to explore the effects of phenotypic differences resulting from acclimation to different growth conditions. Parameters of photosynthesis (P) vs Irradiance (E) curves were estimated by fitting the data to a cumulative one-hit Poisson model pioneered for photosynthesis by Webb et al. (1974):

$$P_{net} = P_g - R_D \quad (1)$$

$$P_{net} = [P_E \cdot \left(1 - e^{-E/E_k}\right)] - R_D \quad (2)$$

where P_{net} was the measured rate of net photosynthesis and R_D was the measured rate of dark respiration, from which the gross photosynthesis (P_g) was calculated according to Equation (1). P_g was defined as a function of light, where P_E represented the light-saturated rate of gross photosynthesis that varied with [CO_2] and [HCO_3^-] (sensu McPherson et al. (2015)). E_k was the irradiance threshold for photosynthetic saturation. E was separately defined as photosynthetically available radiation (PAR = $\sum_{400}^{700} E[\lambda]$) and as photosynthetically utilized radiation (PUR = $\sum_{400}^{700} [E(\lambda) \cdot A(\lambda)]$), where $A(\lambda)$ was the spectral leaf absorptance that integrated the variability of light capture efficiency due to changes in leaf optical properties and pigment content/composition. The quantum yield of oxygen evolution (Φ_{O2}) at different irradiances (in units of mol O_2 mol^{-1} absorbed photon) was calculated by $\Phi_{O2} = P_g/PUR$. Maximum quantum yield was calculated as $\Phi_{max} = P_E/E_{k\ (PUR)}$.

Although Equation (1) represents the typical method for determining gross photosynthesis from measured values of P_{net} and R_D, the model does not separately account for O_2 consumed by photorespiration in the chloroplast. It also assumes that the Mehler Ascorbate Peroxidase pathway does not affect net O_2

TABLE 2 Distribution of dissolved inorganic carbon and dissolved oxygen concentrations in seawater during the incubation measurements of net photosynthesis at different light levels, including dark respiration measurements.

		At the start of light measurements			At the start of dark measurements		
	Target pH	Growth pH 6	Growth pH 7	Growth pH 8	Growth pH 6	Growth pH 7	Growth pH 8
Sample Size	6	7	7	5	7	7	5
	7	6	6	6	6	6	6
	8	5	5	5	5	5	5
Average pH	6	6.09 ± 0.01	6.08 ± 0.01	6.05 ± 0.01	6.09 ± 0.01	6.08 ± 0.01	6.04 ± 0.01
	7	6.91 ± 0.01	6.85 ± 0.02	6.87 ± 0.02	6.91 ± 0.01	6.84 ± 0.02	6.86 ± 0.02
	8	7.94 ± 0.05	7.95 ± 0.01	7.94 ± 0.02	8.00 ± 0.04	7.98 ± 0.01	7.98 ± 0.02
Average [TCO_2] (µmol/L)	6	3712 ± 28	3131 ± 18	3256 ± 48	3727 ± 27	3153 ± 20	3277 ± 49
	7	2218 ± 9	1874 ± 12	1861 ± 10	2217 ± 10	1876 ± 10	1866 ± 11
	8	1857 ± 15	1534 ± 3	1535 ± 5	1837 ± 14	1526 ± 4	1526 ± 5
Average [HCO^-_3] (µmol/L)	6	1963 ± 0.1	1623 ± 0.0	1624 ± 0.1	1963 ± 0.1	1624 ± 0.0	1624 ± 0.1
	7	1943 ± 0.7	1610 ± 0.7	1609 ± 0.7	1943 ± 0.7	1610 ± 0.6	1609 ± 0.7
	8	1742 ± 21	1442 ± 4	1444 ± 7	1714 ± 20	1431 ± 5	1432 ± 7
Average [CO_2] (µmol/L)	6	1748 ± 28	1506 ± 18	1631 ± 48	1762 ± 27	1528 ± 20	1652 ± 48
	7	265 ± 8	258 ± 11	246 ± 10	264 ± 10	260 ± 10	250 ± 11
	8	23 ± 3	18 ± 0.5	19 ± 0.9	19 ± 2	17 ± 0.5	17 ± 0.8
Average [O_2] (µmol/L)	6	209.5 ± 3.1	215.0 ± 3.5	215.9 ± 2.0	212.6 ± 2.3	214.6 ± 3.0	216.0 ± 2.0
	7	214.6 ± 3.0	218.4 ± 4.3	217.5 ± 3.1	215.7 ± 3.4	219.4 ± 3.3	216.3 ± 1.7
	8	206.4 ± 2.4	215.8 ± 2.4	211.8 ± 2.7	212.2 ± 3.3	218.7 ± 1.6	215.4 ± 2.8

All measurements were conducted at 25°C using seawater with salinity of 24 ppt.

exchange even though it may facilitate ATP generation and electron flow, which might be detected by fluorescence measurements (Larkum et al., 2006a). Following the principle explained by Raghavendra (2000) gross photosynthesis (P_g) can be detailed as the difference between true photosynthesis (P_T) and photorespiration (P_R):

$$P_g = P_T - P_R \quad (3)$$

Under CO_2-saturation (i.e., at low pH that increases CO_2:O_2 ratio in seawater, Table 2), P_R should approach a minimum (~ 0), so that P_g will be an approximate estimate of true photosynthetic O_2 production (P_T). In this study, O_2 production rates measured at pH 6 were assumed to approximate the true photosynthesis (P_T) for each growth condition. Therefore, photorespiration was calculated by subtracting the carbon limited P_g measured at pH > 6 from P_g measured at pH 6:

$$P_{R\ [pH>6]} = P_{g\ [pH6]} - P_{g\ [pH>6]} \quad (4)$$

$$P_{g\ [pH>6]} = \left[P_E \cdot \left(1 - e^{-E/E_k}\right)\right]_{[pH>6]} \quad (5)$$

$$P_{g\ [pH6]} = \left[P_m \cdot \left(1 - e^{-E/E_k}\right)\right]_{[pH6]} \quad (6)$$

Thus, P_g approached P_E when saturated by light and flow, and it approached the true physiological capacity (P_m) when saturated by CO_2, light and flow. In this formulation, the limit of P_m is set by availability of cellular components such as enzyme and pigment concentrations that may change under different growth conditions.

Pulsed Amplitude Modulation (PAM) fluorescence measurements were analyzed following the calculations outlined in Baker (2008). The maximum (F_m) and minimum (F_0) fluorescence emissions were measured in the dark after at least 10 min of acclimation while simultaneously measuring respiration. The maximum variable fluorescence yield ($F_v = F_m - F_0$) was used to quantify the maximum quantum yield of fluorescence (F_v/F_m), which is a measure of maximum efficiency at which absorbed light by photosystem II (PSII) can be used for photochemistry. The maximum (F'_m) and minimum fluorescence (F_t) emissions induced by the short saturating pulse of PAM were measured again in the light while simultaneously measuring P_{net}. Based on these emissions under the presence of the actinic background light, the effective quantum yield of PSII (Φ_{PSII}), also known as photochemical quenching, was determined as:

$$\Phi_{PSII} = \left(F'_m - F_t\right) / F'_m \quad (7)$$

Φ_{PSII} provides an estimate of the quantum yield of linear electron flow through PSII at a given irradiance. The other non-radiative energy loss that quenches fluorescence, called Non-Photochemical Quenching (NPQ), results from the dissipation of excess excitation energy as heat *via* the Xanthophyll cycle. NPQ was estimated as:

$$NPQ = \left(F_m - F'_m\right) / F'_m \quad (8)$$

For comparisons among the treatments and incubations, NPQ and Φ_{PSII} at different light levels were fitted to a four-parameter sigmoid curve, which is commonly used for dose response analysis (Motulsky and Christopoulos, 2004), with the following formula:

$$NPQ = NPQ_{min} + \frac{(NPQ_{max} + NPQ_{min})}{1 + (PUR/EC50)^{-H}} \quad (9)$$

where the exponent H was Hill slope that controlled the steepness of the dose-response curve. *EC50* was the *PUR* level required to provoke a response halfway between the baseline and maximum responses. The threshold for NPQ_{max} was constrained to 10 based on literature values (Kalaji et al., 2014).

The electron transport rate (ETR) was estimated from Φ_{PSII} as:

$$ETR\ (\mu mol\ electrons\ m^{-2}s^{-1}) = PUR \cdot F_{II} \cdot \Phi_{PSII} \quad (10)$$

where F_{II} was the fraction of *PUR* captured by PSII and its light harvesting complexes (LHC). The typical value of F_{II} for Chlorophyta and seagrasses is about 0.5 (Figueroa et al., 2003; Larkum et al., 2006a). Photosynthetic parameters of ETR curves (i.e., ETR_{max}, α_{ETR} and $E_{k\ -ETR}$) were calculated by modifying the model of O_2 based *P* vs *E*. curves (Equation 2):

$$ETR = ETR_{max} \cdot \left(1 - e^{-E/E_k}\right) \quad (11)$$

Linear electron flow through PSII is directly related to photosynthetic oxygen production, therefore the gross photosynthesis based on fluorescence measurements ($P_{g\text{-}ETR}$) were estimated from ETR as:

$$P_{g-ETR}\ (\mu mol\ \ O_2\ m^{-2}s^{-1}) = ETR \cdot \tau \quad (12)$$

where τ was the ratio of oxygen evolved per electron generated at PSII. Since four stable charge separations are necessary to generate one mole of O_2 at PSII, τ is equal to 0.25.

Statistical analysis

Effects of growth [CO_2] on pigment content and optical properties of leaves were analyzed by one-way Analysis of Variance (ANOVA) followed by the Tukey multiple comparison method when significant overall effects were identified. Effects of growth [CO_2] and measurement [CO_2] on

dark respiration rates, measured with the O_2 evolution method, were analyzed by Analysis of Covariance (ANCOVA).

O_2 evolution and fluorescence models were implemented by using the non-linear curve fitting tools in SigmaPlot (Systat Software Inc., Version 13.0). This tool provided the mean estimates of the model parameters with their error estimates and significances using computational procedures described by Draper and Smith (1981) and Zimmerman et al. (1987). Additionally, analysis of variance for the regression models were presented to account for the goodness of fit of the *P* vs *E* curves for each experimental condition (Supplementary Tables 1–3). Significant effects of measurement $[CO_2]$ and growth $[CO_2]$ on model parameters obtained by non-linear regression were analyzed by ANCOVA, with growth pH as the primary (categorial) factor and measurement pH as the continuous covariate.

Results

Photoacclimation to growth CO_2

Pigment content and optical properties varied significantly among the leaves grown in different $[CO_2]$ treatments (Table 3). Both total chlorophyll and carotenoid content decreased with increasing growth $[CO_2]$, while the molar ratio of Total Car : Total Chl remained constant across CO_2 treatments at about 0.27. The decrease in total chlorophyll resulted in an increased optical cross section ($a_L^*(\lambda)$) with growth $[CO_2]$, thereby reducing the package effect that results in Chlorophyll self-shading. Growth $[CO_2]$ increased the thickness of the unpigmented mesophyll, thereby increasing the leaf biomass per unit of surface area. These phenotypic responses, consistent with the long term acclimation responses described by Celebi-Ergin et al. (2021), had important consequences for the comparison of photosynthetic efficiencies when metabolic rates were normalized to different leaf properties.

Light response curves of oxygen flux

Rates of dark respiration, whether normalized to biomass ($R_{D\ (FW)}$) or leaf area ($R_{D\ (LA)}$), were not affected by growth $[CO_2]$ or instantaneous variations of $[CO_2]$ within the metabolic incubation chambers (Table 4). Therefore, the average rate of dark respiration for all samples combined was 5.96 ± 0.31 μmol O_2 hr^{-1} g^{-1} FW or 0.50 ± 0.03 μmol O_2 m^{-2} s^{-1}. Dark respiration rates were also independent of pH within the range examined here, indicating no negative impact of changing ionic composition on respiration.

In contrast, net O_2 production rates increased with light and incubation $[CO_2]$ for all plants, regardless of the CO_2 environment in which they were grown (Figure 1). The biomass specific rate of light-saturated photosynthesis ($P_{E\ (FW)}$) averaged 14.1 μmol O_2 hr^{-1} g^{-1} FW at low incubation $[CO_2]$ for all plants and increased as a function of incubation $[CO_2]$ (Figure 1). However, $P_{E\ (FW)}$ of the plants grown under ambient conditions ($G_{pH}8$) was twice as sensitive to increasing incubation $[CO_2]$ as plants grown under the highest CO_2 enrichment ($G_{pH}6$) (Table 5, 86.8 vs 33.5 μmol O_2 hr^{-1} g^{-1} FW at M_{pH} 6 respectively). This difference was associated with 2-fold higher biomass specific pigment content of the plants grown under ambient $[CO_2]$ (Table 3). Thus, low rates of oxygen evolution by ambient plants in their natural low CO_2 environment resulted mainly from photorespiration and not the lack of photosynthetic capacity characterized by light harvesting, electron transport and carbon fixation.

For all plants, increased incubation $[CO_2]$ also increased the irradiance required to saturate photosynthetic oxygen production ($E_{k\ (PAR)}$ and $E_{k\ (PUR)}$); rather than changing the

TABLE 3 Pigment content and optical properties of leaves used in photosynthesis measurements.

Growth pH (Growth $[CO_2]$)	pH8 (55 μM)	pH7 (371 μM)	pH6 (2121 μM)
Sample Size (n)	16	18	18
FW per LA (mg cm^{-2})	25.8 ± 1.33 ^{a}	27.1 ± 0.92 ^{a}	36.0 ± 1.52 ^{b}
Total Chl per LA (µg Chl cm^{-2})	31.2 ± 1.22 ^{a}	27.0 ± 1.20 ^{b}	20.8 ± 0.86 ^{c}
Total Chl per FW (mg Chl g^{-1} FW)	1.25 ± 0.07 ^{a}	1.01 ± 0.05 ^{b}	0.59 ± 0.03 ^{c}
Total Car per LA (µg Car cm^{-2})	8.16 ± 0.28 ^{a}	7.25 ± 0.25 ^{b}	5.61 ± 0.17 ^{c}
Chl a:b	3.44 ± 0.04 ^{a}	3.73 ± 0.07 ^{b}	3.61 ± 0.04 ^{a,b}
TCar:TChl	0.26 ± 0.00 ^{a}	0.27 ± 0.00 ^{a}	0.27 ± 0.00 ^{a}
Absorptance at 550nm	0.38 ± 0.01 ^{a}	0.37 ± 0.01 ^{a}	0.29 ± 0.01 ^{b}
Absorptance at 680nm	0.75 ± 0.01 ^{a,b}	0.75 ± 0.01 ^{a}	0.73 ± 0.01 ^{b}
$a_L^*(680)$ (m^2 g^{-1} Chl)	5.90 ± 0.33 ^{a}	6.73 ± 0.29 ^{a}	8.10 ± 0.24 ^{b}

Effects of growth pH on mean concentrations (± 1 SE) were analyzed by one-way ANOVA. Different letters represent significant differences among the growth pH for each parameter compared by Tukey method at $p< 0.05$. FW, Fresh Weight; LA, Leaf Area; Chl, Chlorophyll; Car, Carotenoid.

TABLE 4 Dark respiration (R_D) rates measured with O_2 evolution method and estimated by non-linear model fit to *P vs E* curves.

Growth pH	Measurement pH	Measured Dark Respiration Averages (μmol O_2 hr^{-1} g^{-1} FW)	Modeled Dark Respiration (μmol O_2 hr^{-1} g^{-1} FW)	Modeled Dark Respiration (μmol O_2 s^{-1} m^{-2})
6	6	4.61 ± 0.75	4.73 ± 1.34	0.45 ± 0.10
	7	5.31 ± 0.62	5.50 ± 1.15	0.51 ± 0.08
	8	5.84 ± 0.47	5.90 ± 0.63	0.69 ± 0.07
7	6	6.40 ± 1.14	6.90 ± 3.06	0.51 ± 0.12
	7	6.73 ± 1.20	7.08 ± 3.02	0.53 ± 0.22
	8	5.03 ± 0.91	5.04 ± 1.88	0.37 ± 0.12
8	6	6.52 ± 0.93	6.83 ± 2.06	0.46 ± 0.07
	7	6.18 ± 0.75	6.71 ± 2.19	0.46 ± 0.14
	8	7.29 ± 1.26	7.29 ± 1.05	0.56 ± 0.10

ANCOVA of Measured R_D	*df*	SS	MS	F	*p*
Growth pH	2	11.551	5.776	1.173	0.318
Measurement pH	1	0.531	0.531	0.108	0.744
Growth pH x Measurement pH	2	10.206	5.103	1.037	0.363
Residual	46	226.435	4.922	–	–
Total	51	255.682	5.013	–	–

Rates are normalized both to Fresh Weight (FW) and Leaf Area. Effects of measurement pH and growth pH on measured R_D were analyzed by ANCOVA. Sample size for each condition is given in Table 2.

photosynthetic efficiency (α) within the light limited region of *P* versus *E* response curves (Table 5 and Supplementary Table 1). Overall, photoacclimation of eelgrass leaves to ocean carbonation increased $E_{k\ (PUR)}$ values from 17 to 44 and 48 μmol absorbed photon s^{-1} m^{-2} for pH 8 (55 μM $CO_{2(aq)}$), pH 7 (371 μM $CO_{2(aq)}$) and pH 6 (2121 μM $CO_{2(aq)}$) respectively.

Chlorophyll specific rates of light-saturated photosynthesis ($P_{E\ (Chl)}$) were the same for all plants grown at different CO_2 environments and produced an identical response to incubation [CO_2] (Figure 2). Consequently, the O_2 production efficiency per unit chlorophyll was not affected by the CO_2 environment in which the plants were grown (Table 5 and Supplementary Table 2) and the stimulatory effect of [CO_2] on O_2 evolution was instantaneous (Figure 3A). The most likely explanation for this instantaneous response would be a reversible and light dependent O_2 consuming process involving the chloroplast, such as photorespiration (P_R), that is competitively inhibited by increasing [CO_2]. Therefore, for all plants grown under all treatments, $P_{E\ (Chl)}$ rates at high incubation [CO_2] (i.e., at $M_{pH}6$) were assumed to be the true physiological photosynthetic capacity (P_m) under light, carbon and flow saturation. Based on this assumption, photorespiration rates were quantified by solving the Equation 4 with the chlorophyll specific gross photosynthesis models (Figure 3B). Normalizing the models to pigment, rather than biomass or area, eliminated the effect of morphological differences among the plants on net oxygen metabolism.

Like photosynthesis, photorespiration increased with light under constant [CO_2], but decreased with increasing incubation [CO_2], as carboxylation became increasingly favored over oxygenation (Figure 3B). Predicted P_R rates increased rapidly with light to a maximum of 60 to 80% of P_m at low [CO_2] (i.e., $M_{pH}8$) (Figure 3C). When aqueous [CO_2] was equal to aqueous [O_2] (at $M_{pH}7$, Table 2), maximum P_R rates were only 20% of P_m, which is equivalent to the inherent carboxylation: oxygenation ratio of Rubisco.

All plants reached the lowest gross photosynthesis to dark respiration ratio (P_g : R_D) of 2 at low incubation [CO_2] when light saturated (Figure 4A). This ratio increased instantaneously when saturated with CO_2 in the incubation medium, maximally up to 12 for ambient plants ($G_{pH}8$). However, the P_E : R_D ratio of high CO_2 grown plants peaked at 8 when saturated with CO_2 in the incubation medium, illustrating the consequence of pigment acclimation on metabolic balance of plants grown in a high CO_2 environment (Figure 4B, grey arrows). Having excess pigment content in a CO_2-limited environment (as observed in ambient plants) did not improve the P_E : R_D under normal growth conditions even though it allowed the instantaneous 6-fold increase of P_E : R_D when incubation [CO_2] increased. High CO_2 acclimated plants, on the other hand, maintained a 4-fold higher P_E : R_D above ambient plants at their respective growth [CO_2] even though pigment content of the high CO_2 plants decreased by half.

Light response curves of variable fluorescence

Maximum quantum yields of fluorescence by dark-adapted leaves were above 0.7 regardless of incubation [CO_2], indicating leaves from all growth treatments were healthy during the experiments (Φ_{PSII} at PUR 0 μmol absorbed photon s^{-1} m^{-2},

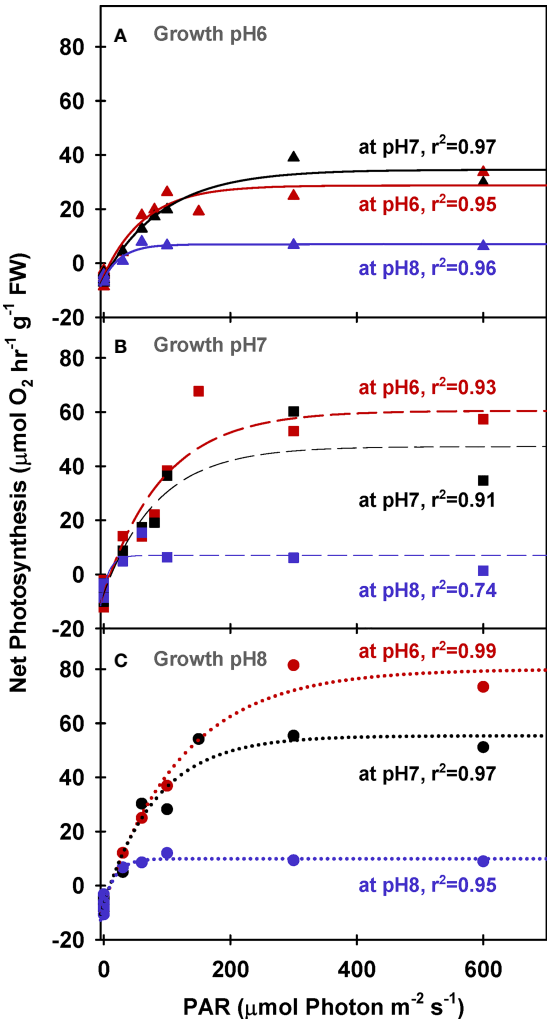

FIGURE 1
Net photosynthesis of eelgrass leaves (biomass normalized) as a function of irradiance. O_2 production rates were measured at different pH levels (red: pH6, black: pH7 and blue: pH8) using leaves grown at pH6 (2121 μM $CO_{2(aq)}$) **(A)**, pH7 (371 μM $CO_{2(aq)}$) **(B)** and ambient pH8 (55 μM $CO_{2(aq)}$) **(C)**. Curves were fit using Equation (2).

Figure 5). For all plants, effective quantum yields of fluorescence (Φ_{PSII}) decreased faster with increasing light when the incubation [CO_2] was low ($M_{pH}8$). The decreased photochemical yield resulted from rapid induction of non-photochemical quenching (NPQ) when [CO_2] was limited under light saturation (Figure 6). Increasing the growth [CO_2], however, caused the light-dependent onset of NPQ to increase, as the NPQ pathway saturated more quickly due the decreased carotenoid content of leaves grown under high [CO_2] (Table 3).

Under saturating irradiance (350 μmol absorbed photon s^{-1} m^{-2}, Figure 6), NPQ values of ambient plants increased 5-fold as incubation [CO_2] became increasingly limiting. In contrast, the plants grown under high [CO_2] ($G_{pH}6$) yielded the same light-saturated NPQ of 2.5 regardless of incubation [CO_2]. The dynamic range of NPQ regulation in ambient grown plants in response to instantaneous changes in [CO_2] suggests considerable tolerance for fluctuating environmental conditions (Figure 6C).

The relation between quantum yield of fluorescence (Φ_{PSII}) and quantum yield of oxygen evolution (Φ_{O2}) was nonlinear, and their ratios were closest to the theoretical value of 8 only at low light and high [CO_2] conditions (Figure 7). For this ratio to be higher than 8, either less than half of the photons are directed to PSII (i.e., F_{II}<0.5, Equation 10), and/or more than four electrons are processed to evolve one mole of oxygen (i.e., τ<0.25, Equation 12). Both outcomes highlight deviation from linear electron flow. For ambient plants, Φ_{O2} decreased faster than Φ_{PSII} with increasing light resulting in a drastic increase in Φ_{PSII}:Φ_{O2}, especially at their growth CO_2 ($G_{pH}8$), suggesting that these plants were using an alternative pathway to maintain electron flow without the production or consumption of O_2.

Similar to net photosynthesis rates, electron transport rates (ETR) of all plants increased with light and were lowest at low incubation [CO_2] (i.e., $M_{pH}8$) (Figure 8 and Table 5). However, the increase of ETR_{max} with incubation CO_2 was not consistent among the plants due to the non-monotonic response of Φ_{PSII} with incubation [CO_2] (Figure 5), in agreement with the findings by Celebi (2016). Only ETR_{max} of plants grown at $G_{pH}7$ increased consistently with increasing incubation [CO_2]. For all incubation experiments, PUR levels required to saturate ETR ($E_{k\text{-}ETR}$) were consistently higher than the E_k values required to saturate O_2 production (Table 5 and Supplementary Table 3). For all plants, estimated gross photosynthesis based on ETR were also higher than the gross photosynthesis measured by the O_2 evolution method (Figure 9). However, this overestimation was not consistent among plants grown at different CO_2 environments. The $P_{E\ (LA)}$ to ETR_{max} ratio was around 0.1 for pH 6 and pH 8 plants when incubated at pH 6 and pH 8, instead of the theoretical value (τ) of 0.25 (Table 5).

Discussion

Long-term growth under high [CO_2] produced a remarkable combination of morphological and metabolic changes in eelgrass. Although pigment content decreased in plants grown at high CO_2, leaf biomass increased as a direct result of the CO_2-stimulated increase in photosynthetic carbon gain. The equivalent responses of chlorophyll normalized O_2 production rates to increased incubation [CO_2], independent of the growth CO_2, allowed us to quantify the impact of [CO_2] on photorespiration in eelgrass because the instantaneous difference in O_2 production rates in CO_2-saturated vs. CO_2-limited incubation media corresponded to the amount of O_2 consumed in the photorespiratory pathway. Thus, photosynthesis and photorespiration as a function of light for

each growth condition were precisely predictable using the *P* versus *E* curves, although the responses to incubation CO_2 differed between biomass and pigment normalization due to changes in leaf morphology. Presently, models of eelgrass performance do not consider these long-term morphological and metabolic acclimation responses (Zimmerman, 2003; Zimmerman, 2006; Zimmerman et al., 2015). Thus, the quasi-mechanistic model developed in this study permits integration of the photosynthetic and morphological acclimation due to ocean carbonation into seagrass productivity models, by adjusting the limits of the photosynthetic parameters based on substrate availability and physiological capacity.

Morphological acclimation and regulation of pigment content, Rubisco activity, light capture and carbon fixation as a function of CO_2 availability have been previously observed in freshwater angiosperms (Madsen et al., 1996). Increasing $P_g : R_D$ due to the enhancing impact of $[CO_2]$ on P_E was detected even in short term (2-6 weeks) studies using temperate and tropical seagrass species without any CO_2 effect on pigment content (Zimmerman et al., 1997; Ow et al., 2015). Long term studies, moreover, reported significant increases in total shoot biomass, carbon allocation to roots and rhizomes (blue carbon), shoot survival and reproductive output by eelgrass in response to CO_2 availability (Palacios and Zimmerman, 2007; Zimmerman et al.,

TABLE 5 Model estimates (mean ± 1 SE) of photosynthesis parameters generated by non-linear regression fit to the experimental data using Equation (2) (N.S. stands for non-significant parameter estimate).

Model Estimates	Growth pH	Measurement pH		
		6.0	7.0	8.0
P_E (μmol O_2 hr^{-1} mg^{-1} Chl)	6	70.2 ± 4.3	55.2 ± 3.7	24.5 ± 2.1
G_{pH} x M_{pH}: p=0.570	7	68.0 ± 3.2	49.3 ± 3.1	12.5 ± 3.1
G_{pH}: p=0.583	8	62.6 ± 2.4	44.9 ± 4.0	20.3 ± 2.4
M_{pH}: p=0.002				
P_E (μmol O_2 hr^{-1} g^{-1} FW)	6	33.5 ± 2.8	40.0 ± 2.5	12.9 ± 1.1
G_{pH} x M_{pH}: p=0.240	7	67.4 ± 7.1	54.3 ± 6.5	12.1 ± 2.9
G_{pH}: p=0.185	8	86.8 ± 4.7	62.1 ± 4.6	17.2 ± 1.7
M_{pH}: p=0.014				
P_E (μmol O_2 s^{-1} m^{-2})	6	3.6 ± 0.2	3.5 ± 0.2	1.5 ± 0.1
G_{pH} x M_{pH}: p=0.233	7	5.8 ± 0.3	4.3 ± 0.5	0.9 ± 0.2
G_{pH}: p=0.199	8	5.8 ± 0.2	4.3 ± 0.3	1.5 ± 0.2
M_{pH}: p=0.007				
ETR_{max} (μmol Electron s^{-1} m^{-2})	6	35.3 ± 0.4	41.0 ± 3.3	22.4 ± 0.5
G_{pH} x M_{pH}: p=0.573	7	93.1 ± 2.6	68.3 ± 4.2	32.4 ± 1.1
G_{pH}: p=0.482	8	58.4 ± 5.8	82.2 ± 5.5	22.8 ± 0.7
M_{pH}: p=0.119				
α_{ETR} (μmol Electron μmol^{-1} absorbed Photon)	6	0.45 ± 0.01	0.50 ± 0.07	0.52 ± 0.03
G_{pH} x M_{pH}: p=0.696	7	0.42 ± 0.01	0.48 ± 0.04	0.44 ± 0.04
G_{pH}: p=0.735	8	0.50 ± 0.08	0.46 ± 0.03	0.52 ± 0.04
M_{pH}: p=0.257				
Φ_{max} (μmol O_2 μmol^{-1} absorbed Photon)	6	0.077 ± 0.01	0.084 ± 0.01	0.107 ± 0.03
G_{pH} x M_{pH}: p=0.263	7	0.079 ± 0.01	0.079 ± 0.02	0.14 ± 0.24
G_{pH}: p=0.314	8	0.083 ± 0.01	0.074 ± 0.01	0.081 ± 0.03
M_{pH}: p=0.100				
E_k (μmol absorbed photon s^{-1} m^{-2}) from 'PG per Chl vs PUR'	6	47.5 ± 7.0	36.4 ± 6.0	14.5 ± 4.9
G_{pH} x M_{pH}: p=0.391	7	64.2 ± 7.4	43.9 ± 6.9	4.7 ± 15.8
G_{pH}: p=0.348	8	68.6 ± 7.2	57.1 ± 13.3	17.4 ± 7.1
M_{pH}: p=0.006				
E_k (μmol photon s^{-1} m^{-2}) from 'PG per FW vs PAR'	6	65.0 ± 14.5	94.7 ± 14.8	28.4 ± 8.6
G_{pH} x M_{pH}: p=0.523	7	94.0 ± 24.2	85.3 ± 25.1	11.6 ± 23.5
G_{pH}: p=0.501	8	124.9 ± 18.6	83.9 ± 16.9	18.3 ± 8.7
M_{pH}: p=0.046				
E_k (μmol absorbed photon s^{-1} m^{-2}) from 'ETR vs PUR'	6	78.5 ± 2.0	82.2 ± 15.6	43.1 ± 2.9
G_{pH} x M_{pH}: p=0.560	7	220.1 ± 10.3	142.6 ± 19.0	72.8 ± 7.3
G_{pH}: p=0.469	8	117.5 ± 27.8	180.1 ± 22.9	44.2 ± 3.8
M_{pH}: p=0.117				

Significant effects of measurement pH (M_{pH}) and growth pH (G_{pH}) on mean estimates were analyzed by ANCOVA.

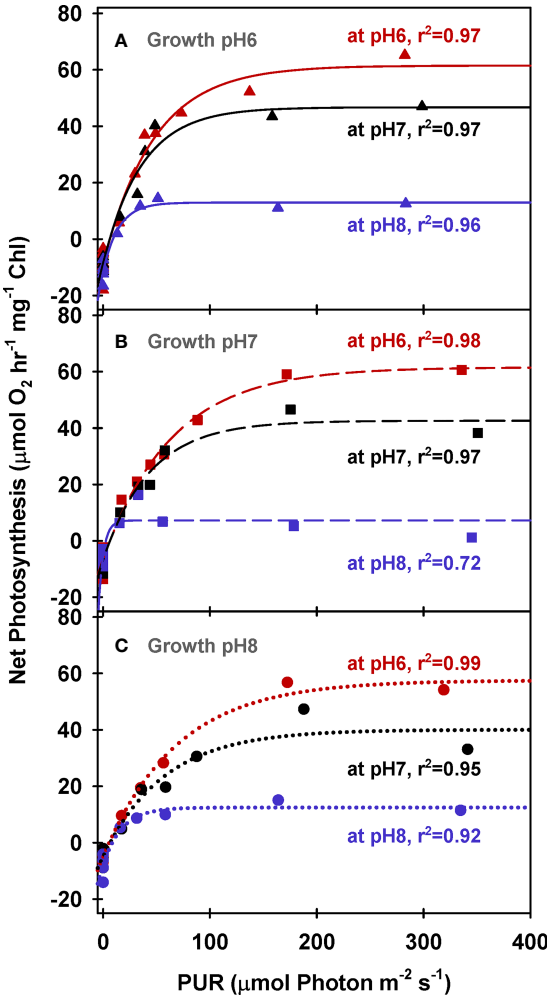

FIGURE 2
Net photosynthesis of eelgrass leaves (Chlorophyll normalized) as a function of absorbed irradiance. O_2 production rates were measured at different pH levels (red: pH6, black: pH7 and blue: pH8) using leaves grown at pH6 (2121 μM $CO_{2(aq)}$) **(A)**, pH7 (371 μM $CO_{2(aq)}$) **(B)** and ambient pH8 (55 μM $CO_{2(aq)}$) **(C)**. Curves were fit using Equation (2).

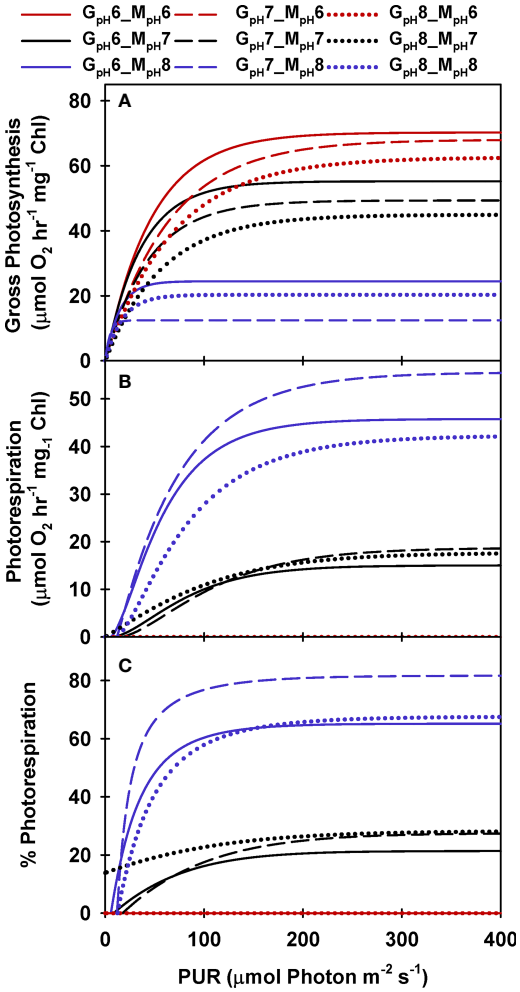

FIGURE 3
Modeled gross photosynthesis **(A)** and photorespiration **(B, C)** of eelgrass leaves as a function of absorbed irradiance. Colors represent different pH/CO_2 levels at which the measurements (M_{pH}) were performed; line styles represent the different pH/CO_2 levels at which the plants were grown (G_{pH}). Photorespiration at M_{pH6} were zero.

2017). Despite the decreases in pigment content and leaf absorptance observed here, plants grown at high CO_2 were able to maintain higher P_g : R_D ratios than plants grown under ambient CO_2; indicating a strong coupling between the regulation of photosynthetic structure and metabolic carbon demands. This coupling between photosynthetic regulation and growth might be poor for organisms that undergo photodamage because photosynthesis might accommodate the biochemical costs associated with protection and recovery rather than fueling the energy towards growth (Barra et al., 2014). On the other hand, the eelgrass used in these experiments show no sign of photodamage, either in the growth aquaria or in laboratory incubations even when photosynthesis was carbon limited but light saturated.

When measured at low [CO_2], plants grown under ambient CO_2 had the same photosynthetic O_2 production as the plants grown at high [CO_2]. These same photosynthetic rates highlighted the apparent lack of carbon concentrating mechanisms inducible by low CO_2 availability in eelgrass, in contrast with marine algae and cyanobacteria that are capable of upregulating their carbon concentrating mechanisms *via* e.g., generation of pyrenoids, carboxysomes and periplasmic carbonic anhydrases when CO_2 availability becomes limiting (Björk et al., 1993; Raghavendra, 2000; Falkowski and Raven, 2007; Meyer et al., 2017). This was also consistent with the

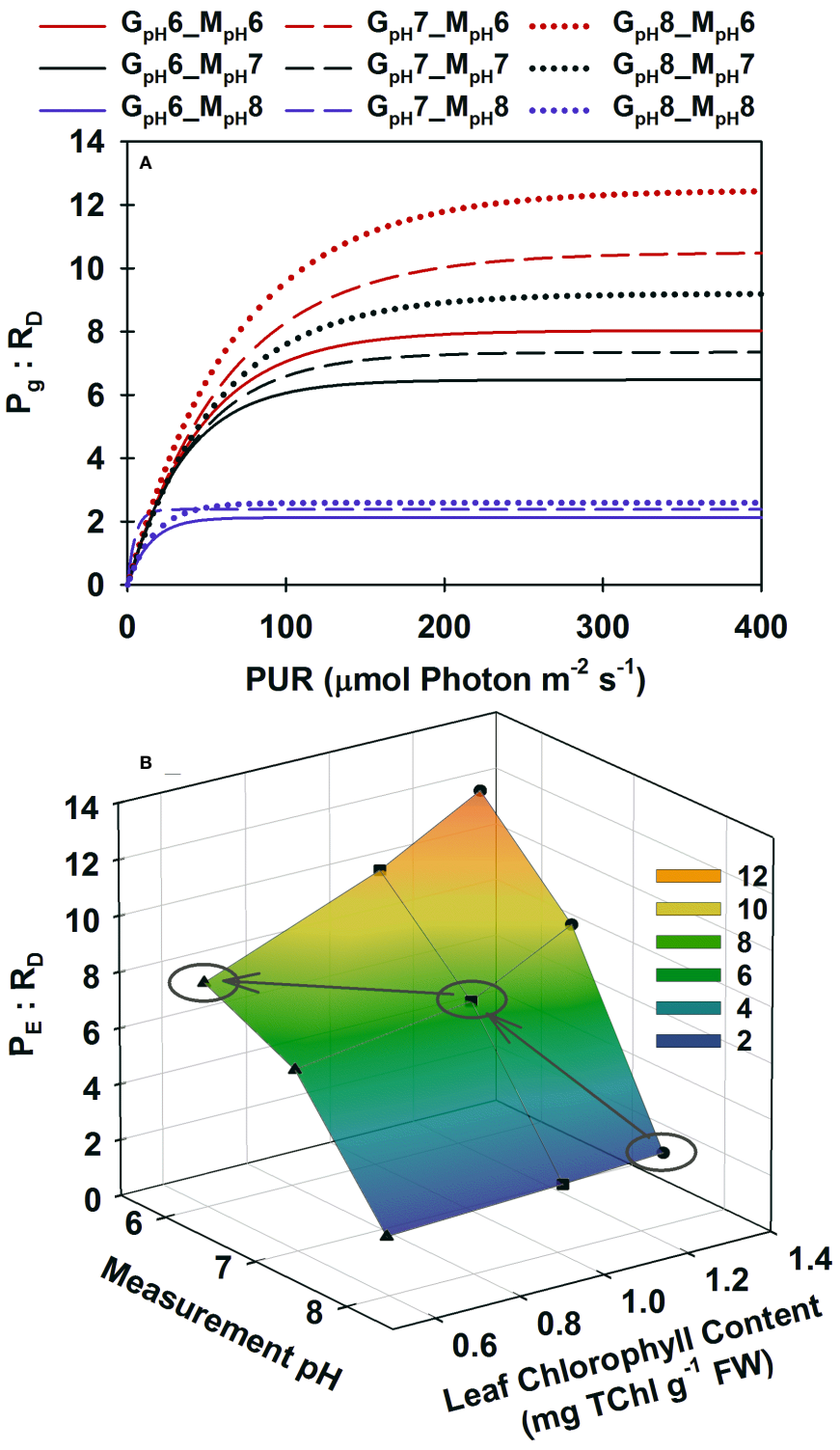

FIGURE 4
Modeled ratio of gross photosynthesis to dark respiration as a function of absorbed irradiance **(A)** and as a function of Chlorophyll content at saturating irradiances **(B)**. Colors represent different pH/CO_2 levels at which the measurements (M_{pH}) were performed; line styles and symbols (▲, at pH6 ■ at pH7, ● at ambient pH) represent the different pH/CO_2 levels at which the plants were grown (G_{pH}). **(B)** Ellipses highlight when plants from different treatments were incubated at their corresponding growth pH/CO_2. Gray arrows show the trajectory of $P_E : R_D$ as a result of phenotypic acclimation to the increasing CO_2 environment.

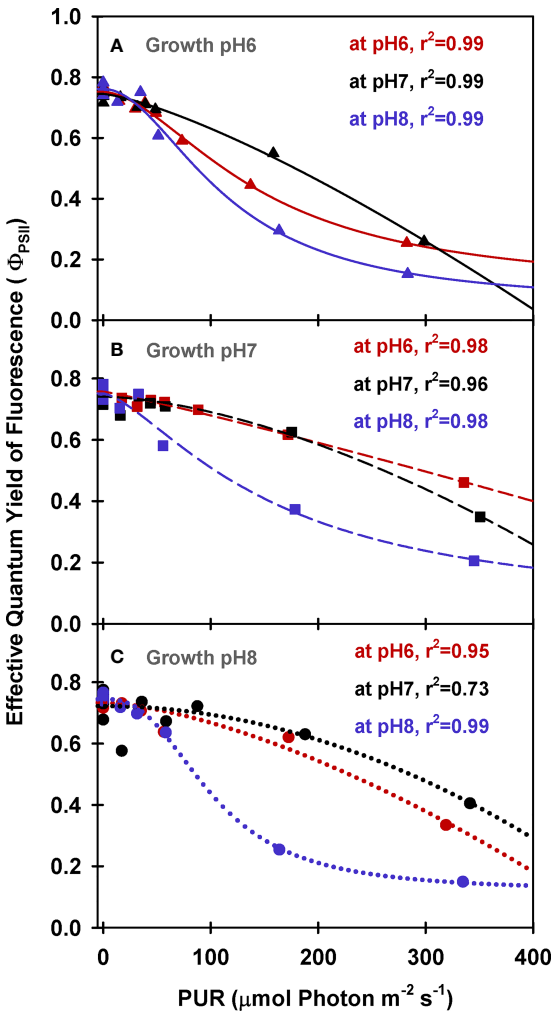

FIGURE 5
PAM fluorescence parameters of eelgrass leaves as a function of absorbed irradiance. PAM fluorescence measurements were performed at different pH/CO_2 levels (red: pH6, black: pH7, blue: pH8) using leaves grown at pH6 (2121 μM $CO_{2(aq)}$) **(A)**, pH7 (371 μM $CO_{2(aq)}$) **(B)** and ambient pH8 (55 μM $CO_{2(aq)}$) **(C)**. Curves were fit using Equation (9).

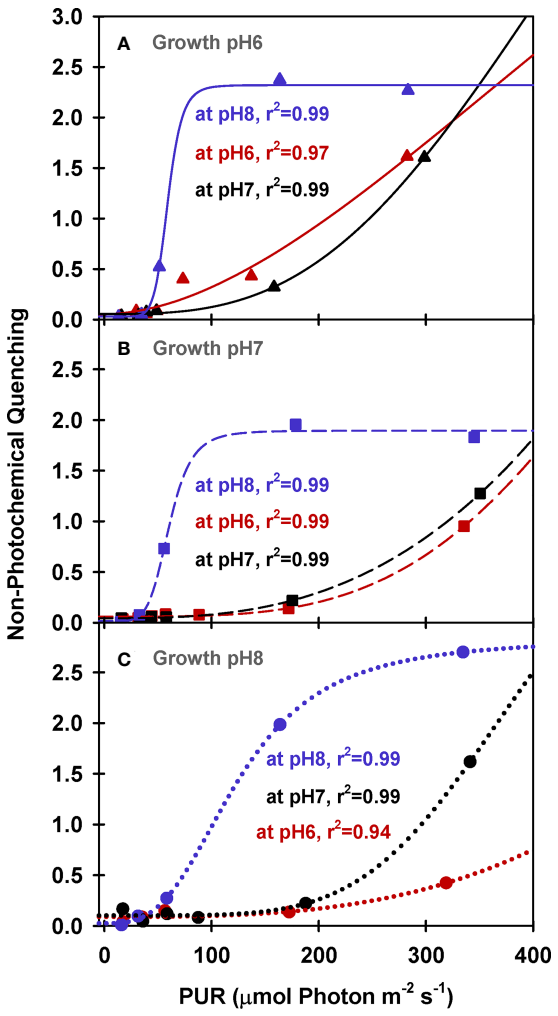

FIGURE 6
PAM fluorescence parameters of eelgrass leaves as a function of absorbed irradiance. PAM fluorescence measurements were performed at different pH/CO_2 levels (red: pH6, black: pH7, blue: pH8) using leaves grown at pH6 (2121 μM $CO_{2(aq)}$) **(A)**, pH7 (371 μM $CO_{2(aq)}$) **(B)** and ambient pH8 (55 μM $CO_{2(aq)}$) **(C)**. Curves were fit using Equation (9).

limited sensitivity of eelgrass photosynthesis to the aqueous presence of acetazolamide, an inhibitor of periplasmic carbonic anhydrase (McPherson et al. (2015) and Celebi-Ergin - unpublished data). Seagrasses living in shallow estuarine environments, like the Chesapeake Bay eelgrass used in this study, are subject to highly variable CO_2/pH levels daily and seasonally, which might explain the unresponsiveness of CCMs for ambient plants (Buapet et al., 2013a; Duarte et al., 2013; Ruesink et al., 2015; Zimmerman et al., 2017; Cyronak et al., 2018). Similarly, all plants had the same $P_{E\ (Chl)}$ when measured at saturating [CO_2] due to minimized P_R, indicating all plants approached the same physiological oxygen production capacity per available photosynthetic apparatus (i.e., $P_{m\ (Chl)}$ was constant across all treatments). Therefore, the difference in P_E : R_D among growth [CO_2] treatments when all were incubated at high [CO_2] resulted from the downregulation of light harvesting components by plants grown in the high CO_2 environment.

Despite phenotypic acclimation across the CO_2 gradient, the maximum photosynthetic efficiency (Φ_{max}) remained constant for all plants (~0.08 mol O_2 mol^{-1} absorbed photon) but photosynthesis-saturating light levels (E_k) increased, as was predicted by the model of McPherson et al. (2015). Photosynthetic efficiency within and among seagrass species vary with efficiency of light absorption and the subsequent conversion of that energy into carbon assimilation (Ralph et al., 2007). Although the observed values of α in this study

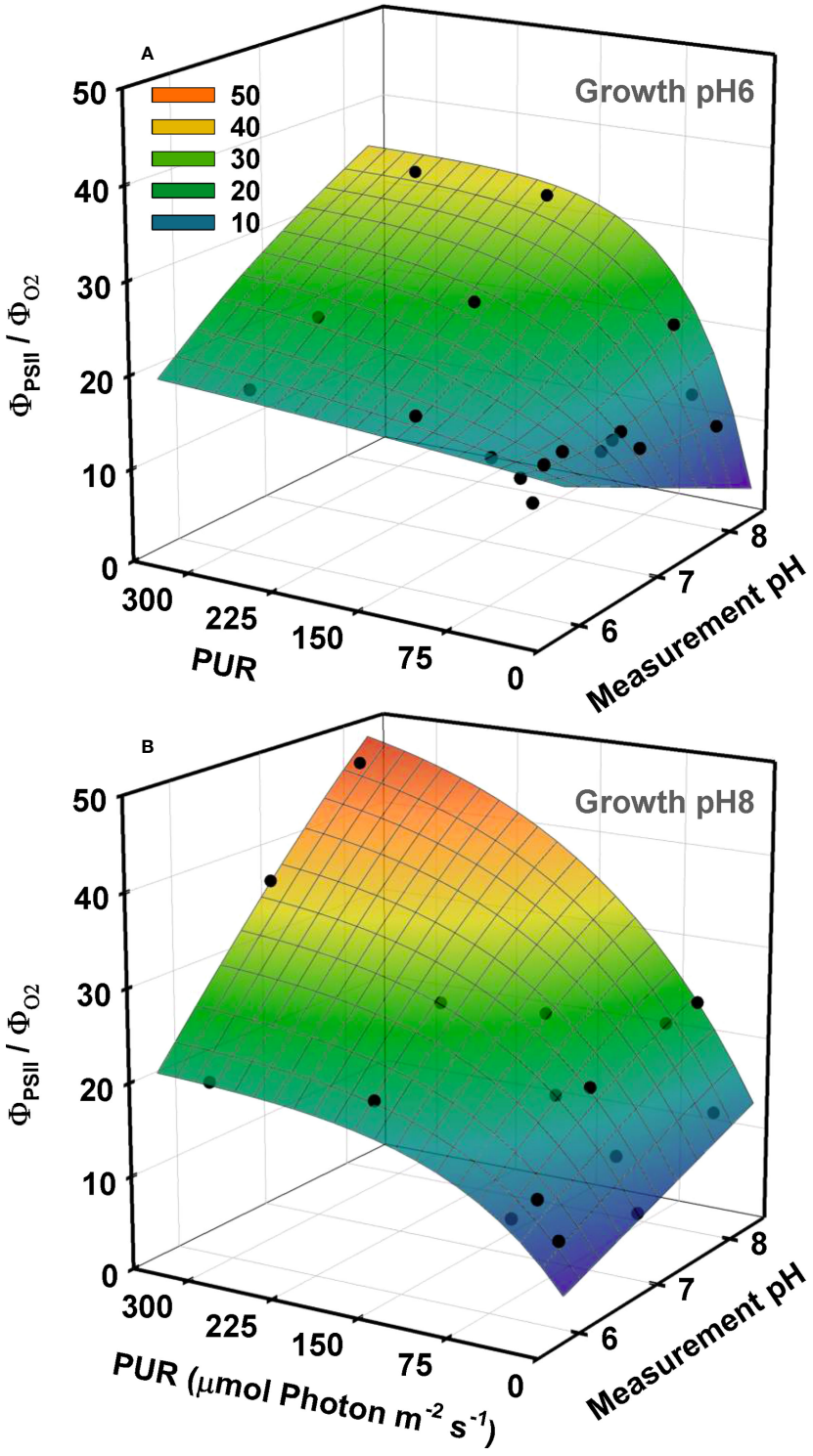

FIGURE 7
Ratio of the quantum yield of fluorescence (Φ_{PSII}) to the quantum yield of oxygen (Φ_{O2}) as a function of light and incubation pH/CO_2. O_2 production and fluorescence were measured simultaneously at different pH levels using eelgrass leaves grown at different CO_2 treatments. Yields were calculated using PUR. Growth specific 3D relationships, at pH6 (2121 μM $CO_{2(aq)}$) **(A)** and ambient pH8 (55 μM $CO_{2(aq)}$) **(B)**, were generated by the combination of non-linear and linear regression fits. First, the Φ_{PSII}/Φ_{O2} ratio as a function of PUR were described by the exponential rise to maximum models separately for each incubation pH/CO_2. Parameter estimates of these non-linear regression models were fitted as a function of incubation pH using linear regression.

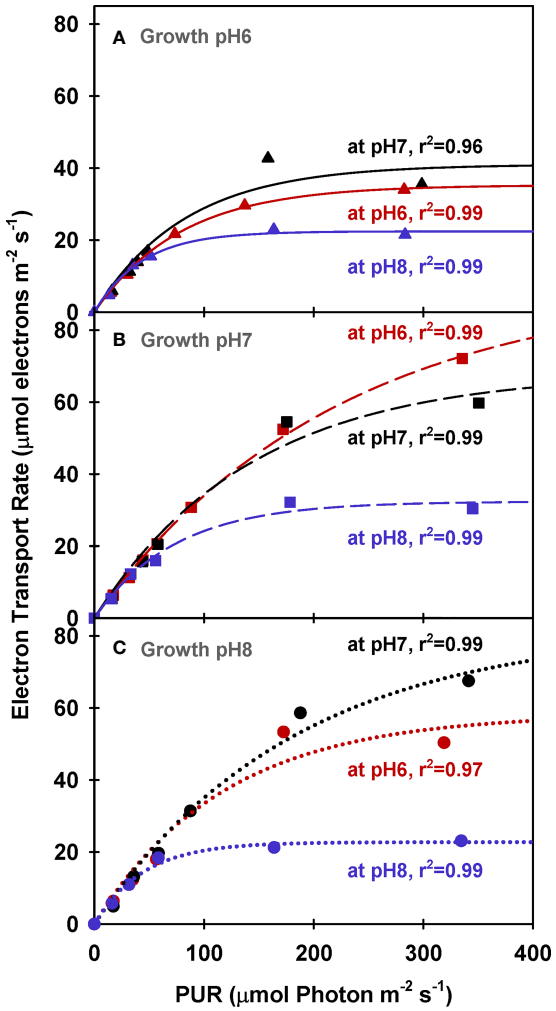

FIGURE 8
Electron transport rates of eelgrass leaves as a function of absorbed irradiance. PAM measurements were performed at different pH/CO_2 levels (red: pH6, black: pH7 and blue: pH8) using leaves grown at pH6 (2121 μM $CO_{2(aq)}$) **(A)**, pH7 (371 μM $CO_{2(aq)}$) **(B)** and ambient pH8 (55 μM $CO_{2(aq)}$) **(C)**. Curves were fit using Equation (11).

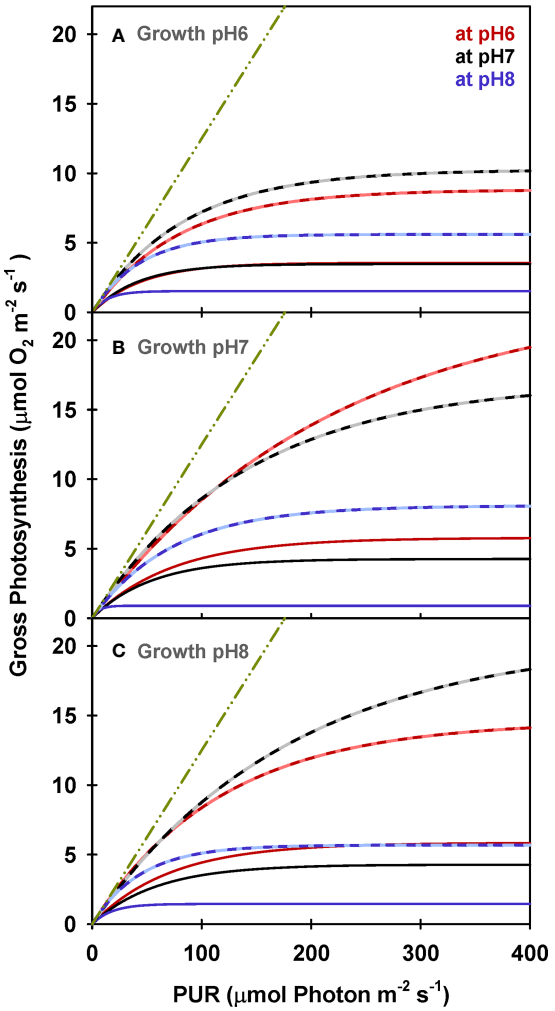

FIGURE 9
Modeled gross photosynthesis of eelgrass leaves as a function of absorbed irradiance for plants growing at pH6 (2121 μM $CO_{2(aq)}$) **(A)**, pH7 (371 μM $CO_{2(aq)}$) **(B)** and ambient pH8 (55 μM $CO_{2(aq)}$) **(C)**. Solid lines are calculated from leaf area normalized O_2 production rates (Equation 1) and dashed lines are estimated from ETR measurements (Equation 12). Colors represent incubation pH/CO_2 levels. Green dot-dashed lines represent the theoretical O_2 production per absorbed photon under non-limiting environmental conditions.

were in agreement with previous estimates for eelgrass (Frost-Christensen and Sand-Jensen, 1992), constant α across different CO_2 regimes represents an interesting contrast to that observed in terrestrial C3 plants in which α increases with [CO_2] availability (Raghavendra, 2000). This difference between responses of aquatic and terrestrial plants may result because CO_2 responses are coupled to water stress in terrestrial plants but not in aquatic plants. The increased E_k and P_E values for high CO_2 acclimated plants will decrease the estimates of H_{sat} (i.e., average daily period of P_E) required to maintain positive carbon balance for the whole plant. The H_{sat} requirement is a useful modeling tool in predicting the depth distribution of eelgrass in variable light environments (Dennison, 1987; Zimmerman et al., 1991; Zimmerman et al., 1994; Zimmerman et al., 1995).

A strong correlation between diurnal NPQ cycle (i.e., xanthophyll cycle) and high light exposure has been confirmed for eelgrass to avoid photodamage under fluctuating light environments (Ralph et al., 2002). High light acclimated eelgrass leaves have higher NPQ activity, and higher photosynthetic capacity, than low light acclimated leaves (Ralph and Gademann, 2005). Here, we demonstrated a similar effect of [CO_2] availability on NPQ activity. Under ambient CO_2 concentrations, the onset of photosynthesis CO_2 limitation (E_k)

occurred at lower irradiance, accelerating the diversion of excess photon absorption to NPQ, likely using the xanthophyll cycle as a photoprotective mechanism to prevent photoinhibition. The high CO_2 incubations reduced this carbon limitation and increased the E_k, consequently reducing NPQ. Due to increased E_k, the same light environment became less damaging at high CO_2, which may explain the reduction in both photosynthetic and photoprotective pigments observed in response to growth CO_2. Thus, by reducing CO_2 limitation of Rubisco, ocean carbonation should also reduce the vulnerability of eelgrass to excess reactive oxygen species (ROS) and therefore the need for photoprotection.

The simultaneous measurements of variable fluorescence, and O_2 flux performed here yielded quantitative estimates of changes in photoprotective pathways of eelgrass acclimated to different CO_2 environments. The difference between the theoretical O_2 evolution (i.e., the linear increase of O_2 with light) and the ETR estimates of gross photosynthesis ($P_{g\text{-}ETR}$) was most pronounced for plants grown at high CO_2, accounting for the absorbed photons that did not contribute to the electron transport pathway (not exciting electrons at PSII), but explained by quenching pathways, such as fluorescence and NPQ. This trend was consistent with their lower area-specific O_2 production rates at high CO_2 incubations when compared to pH7 and ambient pH grown plants. These plants downregulated their pigment content but increased the light-dependent NPQ at lower irradiances even at high incubation [CO_2]. This may indicate that phenotypic acclimation to ocean carbonation by downregulating the photosynthetic apparatus reduces the role of photorespiration but increases the role of NPQ in photoprotection.

On the other hand, as observed in all treatments, the difference between the ETR estimated gross photosynthesis ($P_{g\text{-}ETR}$) and the gross photosynthesis measured by oxygen production (P_g) may result from inaccurate assumptions of F_{ii} and/or τ (Equation 12). In theory, 8 photons absorbed equivalently both by PSI and PSII (F_{ii}= 0.5) excites a total of 4 electrons producing 1 mole of O_2 (τ =0.25). This equilibrium of linear electron flow is valid when there is no limitation of resources such as CO_2 and/or accumulation of byproducts such as reducing equivalents and ROS (Scheibe et al., 2005; Dietz and Pfannschmidt, 2011; Pfannschmidt and Yang, 2012). Under limiting conditions, this balance shifts towards pathways that ensure the optimal redox state of the chloroplast resulting in altered photon: electron: O_2 ratios (Foyer et al., 2012).

Following the linear assumption that 4 electrons produce 1 O_2 (τ = 0.25) resulted in overestimation of the PG_{ETR} in all treatments. Since the molecular chemistry of water splitting at PSII is well-known, τ can only be reduced in an apparent sense. This apparent ratio can result from the excitation of four electrons (as detected with PAM) either without producing O_2, indicating cyclic electron flow around PSII, or consumption of O_2 in the chloroplast that would remain undetected by the gas exchange method (Foyer et al., 2009; Ananyev et al., 2017). Two possible pathways to explain a reduction in τ due to O_2 consumption are (i) the Mehler reaction and (ii) photorespiration. The Mehler reaction increases the pH gradient that may induce NPQ (Demmig-Adams and Adams, 1996; Kanazawa and Kramer, 2002). However, in this study NPQ induction did not happen until Φ_{PSII} values fell below 0.6 while O_2 yield continuously decreased. Therefore, the observed nonlinearity between quantum yield of fluorescence and quantum yield of oxygen most likely resulted from O_2 consumption *via* photorespiration, which probably represents the primary pathway to remove excess O_2 buildup and use the ATP energy from light reactions for this purpose. NPQ was then triggered when photorespiration is incapable of consuming enough ATP to lower the pH gradient forming across lumen at very high irradiances.

Other pathways that keep the electron flow continuous without contributing to CO_2 assimilation are the malate valve and the cyclic electron flow around PSI, which triggers NPQ by generating a pH gradient (Munekage et al., 2004; Johnson, 2005; Miyake, 2010). If PSI cyclic electron flow plays an important role, then the assumption of half of the absorbed photons going to PSII (e.g., F_{ii}=0.5) would be inaccurate. Although PAM measurements are easily made under field conditions (including underwater) and provide non-intrusive information about the photoprotection of eelgrass through NPQ, the fluorescence measurements with PAM overestimate $P_{g\text{-}ETR}$ and therefore are not equivalent to true carbon assimilation. Fluorescence measurements may account for the number of absorbed photons used in electron excitation but not necessarily towards the rates of oxygen production/consumption or carbon assimilation, especially when alternative electron sinks are available (Beer et al., 1998). Still, by having quantified the ratio of Φ_{PSII} to Φ_{O2} as a function of light and carbon availability in response to acclimation to ocean carbonation, the alternative electron pathways can be accounted for in the future estimation of photosynthesis in eelgrass.

To conclude, photorespiration likely provides an important metabolic clutch to protect the photochemical pathway in CO_2-limited eelgrass by maintaining electron flow to prevent the inhibitory damage to photosystems due to light saturation when carbon assimilation is limited by CO_2 supply. In addition to providing a photoprotective role, photorespiration could serve multiple purposes by connecting different metabolic pathways that allow instantaneous energy and reductant modulation under fluctuating environmental conditions. Further, photorespiration may provide a carbon concentrating mechanism *via* recycling of photorespired CO_2 and removing excess intracellular O_2. Therefore, even though carbon limitation causes eelgrass photosynthesis to saturate at relatively low light levels in the modern ocean, longer daily periods of saturating irradiances might be required to keep the photosynthetic apparatus running to produce ATP to support photorespiration. Consequently, understanding photoprotection mechanisms employed by these remarkable plants that are permanently rooted in highly variable shallow-water environments, becomes important when high water

column productivity causes [O_2] to rise and [CO_2] to fall just as daily irradiances begin to peak. More importantly, this study demonstrated that acclimation of photoprotective mechanisms in response to CO_2 availability accounted for the previously reported physiological acclimations of enhanced growth and survival of this species under ocean acidification scenarios.

Data availability statement

The original contributions presented in the study are included in the article/Supplementary Material. Further inquiries can be directed to the corresponding author.

Author contributions

BC-E, RZ and VH conceived the project. BC-E, RZ and VH performed the research. BC-E and RZ analyzed the data. BC-E, RZ and VH wrote the article. All authors contributed to the article and approved the submitted version.

Funding

Financial support for this research was provided by the National Science Foundation (Award OCE-1061823 to RZ and VH), Virginia Sea Grant/NOAA (Award NA14OAR4170093 to RZ and BC-E) and the Department of Ocean, Earth & Atmospheric Sciences, Old Dominion University (to BC-E). This research was performed in partial completion of the requirements for the Ph.D. degree (Oceanography) at Old Dominion University.

Acknowledgments

Thanks to W. M. Swingle and the staff of the Virginia Aquarium & Marine Science Center for assistance with maintenance of the experimental facility, and to D. Ruble, M. Jinuntuya, C. Zayas-Santiago, T. Cedeno and M. Smith for assistance with experimental procedures and maintenance of the experimental plants.

Conflict of interest

The authors declare that the research was conducted in the absence of any commercial or financial relationships that could be construed as a potential conflict of interest.

Publisher's note

Supplementary material

The Supplementary Material for this article can be found online at: https://www.frontiersin.org/articles/10.3389/fpls.2022.1025416/full#supplementary-material

References

Ananyev, G., Gates, C., Kaplan, A., and Dismukes, G. C. (2017). Photosystem II-cyclic electron flow powers exceptional photoprotection and record growth in the microalga chlorella ohadii. *Biochim. Biophys. Acta (BBA) - Bioenergetics* 1858 (11), 873–883. doi: 10.1016/j.bbabio.2017.07.001

Andrews, T. J., and Abel, K. M. (1979). Photosynthetic carbon metabolism in seagrasses 14C-labeling evidence for the C3 pathway. *Plant Physiol.* 63 (4), 650–656. doi: 10.1104/pp.63.4.650

Andrews, T. J., and Lorimer, G. H. (1978). Photorespiration – still unavoidable? *FEBS Lett.* 90 (1), 1–9. doi: 10.1016/0014-5793(78)80286-5

Baker, N. R. (2008). Chlorophyll fluorescence: A probe of photosynthesis *In vivo*. *Annu. Rev. Plant Biol.* 59 (1), 89–113. doi: 10.1146/annurev.arplant.59.032607.092759

Barra, L., Chandrasekaran, R., Corato, F., and Brunet, C. (2014). The challenge of ecophysiological biodiversity for biotechnological applications of marine microalgae. *Mar. Drugs* 12 (3), 1641. doi: 10.3390/md12031641

Bathellier, C., Tcherkez, G., Lorimer, G. H., and Farquhar, G. D. (2018). Rubisco is not really so bad. *Plant Cell Environ.* 41 (4), 705–716. doi: 10.1111/pce.13149

Beer, S., and Koch, E. (1996). Photosynthesis of marine macroalgae and seagrasses in globally changing CO_2 environments. *Mar. Ecol. Prog. Ser.* 141, 199–204. doi: 10.3354/meps141199

Beer, S., Sand-Jensen, K., Madsen, T. V., and Nielsen, S. L. (1991). The carboxylase activity of rubisco and the photosynthetic performance in aquatic plants. *Oecologia* 87 (3), 429–434. doi: 10.1007/BF00634602

Beer, S., Vilenkin, B., Weil, A., Veste, M., Susel, L., and Eshel, A. (1998). Measuring photosynthetic rates in seagrasses by pulse amplitude modulated (PAM) fluorometry. *Mar. Ecology-Progress Ser.* 174, 293–300. doi: 10.3354/meps174293

Björk, M., Haglund, K., Ramazanov, Z., and Pedersén, M. (1993). Inducible mechanisms for HCO_3^- utilization and repression of photorespiration in protoplasts and thalli of three species of ulva (chlorophyta)1. *J. Phycology* 29 (2), 166–173. doi: 10.1111/j.0022-3646.1993.00166.x

Black, C., Burris, J., and Everson, R. (1976). Influence of oxygen concentration on photosynthesis in marine plants. *Funct. Plant Biol.* 3 (1), 81–86. doi: 10.1071/PP9760081

Borum, J., Sand-Jensen, K., Binzer, T., Pedersen, O., and Greve, T. (2006). "Oxygen movement in seagrasses," in *SEAGRASSES: BIOLOGY, ECOLOGYAND CONSERVATION* (Springer, Dordrecht: Springer Netherlands), 255–270. doi: 10.1007/978-1-4020-2983-7_10

Buapet, P., and Björk, M. (2016). The role of O2 as an electron acceptor alternative to CO2 in photosynthesis of the common marine angiosperm zostera marina l. *Photosynthesis Res.* 129 (1), 59–69. doi: 10.1007/s11120-016-0268-4

Buapet, P., Gullström, M., and Björk, M. (2013a). Photosynthetic activity of seagrasses and macroalgae in temperate shallow waters can alter seawater pH and total inorganic carbon content at the scale of a coastal embayment. *Mar. Freshw. Res.* 64 (11), 1040–1048. doi: 10.1071/MF12124

Buapet, P., Rasmusson, L. M., Gullström, M., and Björk, M. (2013b). Photorespiration and carbon limitation determine productivity in temperate seagrasses. *PloS One* 8 (12), e83804. doi: 10.1371/journal.pone.0083804

Burris, J., Holm-Hansen, O., and Black, C. (1976). Glycine and serine production in marine plants as a measure of photorespiration. *Funct. Plant Biol.* 3 (1), 87–92. doi: 10.1071/PP9760087

Busch, F. A., Sage, T. L., Cousins, A. B., and Sage, R. F. (2013). C3 plants enhance rates of photosynthesis by reassimilating photorespired and respired CO_2. *Plant Cell Environ.* 36 (1), 200–212. doi: 10.1111/j.1365-3040.2012.02567.x

Celebi, B. (2016). *Potential impacts of climate change on photochemistry of zostera Marina L.* Doctor of Philosophy (PhD), Dissertation, Ocean & Earth Sciences, (Norfolk, VA: Old Dominion University). doi: 10.25777/8b9x-8303

Celebi-Ergin, B., Zimmerman, R. C., and Hill, V. J. (2021). Impact of ocean carbonation on long-term regulation of light harvesting in eelgrass, *Zostera marina* l. *Mar. Ecol. Prog. Ser.* 671, 111–128. doi: 10.3354/meps13777

Cummings, M. E., and Zimmerman, R. C. (2003). Light harvesting and the package effect in the seagrasses *Thalassia testudinum* banks ex könig and *Zostera marina* l.: optical constraints on photoacclimation. *Aquat. Bot.* 75 (3), 261–274. doi: 10.1016/s0304-3770(02)00180-8

Cyronak, T., Andersson, A. J., D'Angelo, S., Bresnahan, P., Davidson, C., Griffin, A., et al. (2018). Short-term spatial and temporal carbonate chemistry variability in two contrasting seagrass meadows: Implications for pH buffering capacities. *Estuaries Coasts*. 41, 1282–1296. doi: 10.1007/s12237-017-0356-5

Demmig-Adams, B., and Adams, W. W.III (1996). The role of xanthophyll cycle carotenoids in the protection of photosynthesis. *Trends Plant Sci.* 1 (1), 21–26. doi: 10.1016/s1360-1385(96)80019-7

Dennison, W. C. (1987). Effects of light on seagrass photosynthesis, growth and depth distribution. *Aquat. Bot.* 27 (1), 15–26. doi: 10.1016/0304-3770(87)90083-0

Dietz, K.-J., and Pfannschmidt, T. (2011). Novel regulators in photosynthetic redox control of plant metabolism and gene expression. *Plant Physiol.* 155 (4), 1477–1485. doi: 10.1104/pp.110.170043

Downton, W., Bishop, D., Larkum, A., and Osmond, C. (1976). Oxygen inhibition of photosynthetic oxygen evolution in marine plants. *Funct. Plant Biol.* 3 (1), 73–79. doi: 10.1071/PP9760073

Draper, N. R., and Smith, H. (1981). *Applied regression analysis 2nd* Edition (New York: John Wiley & Sons).

Duarte, C. M., Hendriks, I. E., Moore, T. S., Olsen, Y. S., Steckbauer, A., Ramajo, L., et al. (2013). Is ocean acidification an open-ocean syndrome? understanding anthropogenic impacts on seawater pH. *Estuaries Coasts* 36 (2), 221–236. doi: 10.1007/s12237-013-9594-3

Durako, M. J. (1993). Photosynthetic utilization of $CO_{2(aq)}$ and HCO_3^- in *Thalassia testudinum* (Hydrocharitaceae). *Mar. Biol.* 115 (3), 373–380. doi: 10.1007/bf00349834

Falkowski, P. G., and Raven, J. A. (2007). *Aquatic photosynthesis* (Dordrecht: Princeton University Press).

Figueroa, F., Conde-Álvarez, R., and Gómez, I. (2003). Relations between electron transport rates determined by pulse amplitude modulated chlorophyll fluorescence and oxygen evolution in macroalgae under different light conditions. *Photosynthesis Res.* 75 (3), 259–275. doi: 10.1023/A:1023936313544

Foyer, C. H., Bloom, A. J., Queval, G., and Noctor, G. (2009). Photorespiratory metabolism: Genes, mutants, energetics, and redox signaling. *Annu. Rev. Plant Biol.* 60 (1), 455–484. doi: 10.1146/annurev.arplant.043008.091948

Foyer, C. H., Neukermans, J., Queval, G., Noctor, G., and Harbinson, J. (2012). Photosynthetic control of electron transport and the regulation of gene expression. *J. Exp. Bot.* 63 (4), 1637–1661. doi: 10.1093/jxb/ers013

Frost-Christensen, H., and Sand-Jensen, K. (1992). The quantum efficiency of photosynthesis in macroalgae and submerged angiosperms. *Oecologia* 91 (3), 377–384. doi: 10.1007/bf00317627

Heber, U., and Krause, G. H. (1980). What is the physiological role of photorespiration? *Trends Biochem. Sci.* 5 (2), 32–34. doi: 10.1016/s0968-0004(80)80091-0

Hough, R. A. (1974). Photorespiration and productivity in submersed aquatic vascular plants. *Limnology Oceanography* 19 (6), 912–927. doi: 10.4319/lo.1974.19.6.0912

Hough, A. R., and Wetzel, R. G. (1977). Photosynthetic pathways of some aquatic plants. *Aquat. Bot.* 3, 297–313. doi: 10.1016/0304-3770(77)90035-3

Igamberdiev, A. U., Bykova, N. V., Lea, P. J., and Gardestrom, P. (2001). The role of photorespiration in redox and energy balance of photosynthetic plant cells: A study with a barley mutant deficient in glycine decarboxylase. *Physiol. Plant* 111 (4), 427–438. doi: 10.1034/j.1399-3054.2001.1110402.x

Invers, O., Zimmerman, R. C., Alberte, R. S., Pérez, M., and Romero, J. (2001). Inorganic carbon sources for seagrass photosynthesis: an experimental evaluation of bicarbonate use in species inhabiting temperate waters. *J. Exp. Mar. Biol. Ecol.* 265 (2), 203–217. doi: 10.1016/s0022-0981(01)00332-x

Johnson, G. N. (2005). Cyclic electron transport in C3 plants: fact or artefact? *J. Exp. Bot.* 56 (411), 407–416. doi: 10.1093/jxb/eri106

Kalaji, H. M., Schansker, G., Ladle, R. J., Goltsev, V., Bosa, K., Allakhverdiev, S. I., et al. (2014). Frequently asked questions about *in vivo* chlorophyll fluorescence: practical issues. *Photosynthesis Res.* 122 (2), 121–158. doi: 10.1007/s11120-014-0024-6

Kanazawa, A., and Kramer, D. M. (2002). *In vivo* modulation of nonphotochemical exciton quenching (NPQ) by regulation of the chloroplast ATP synthase. *Proc. Natl. Acad. Sci.* 99 (20), 12789–12794. doi: 10.1073/pnas.182427499

Koch, M., Bowes, G., Ross, C., and Zhang, X.-H. (2013). Climate change and ocean acidification effects on seagrasses and marine macroalgae. *Global Change Biol.* 19 (1), 103–132. doi: 10.1111/j.1365-2486.2012.02791.x

Kuypers, M. M. M., Pancost, R. D., and Damste, J. S. S. (1999). A large and abrupt fall in atmospheric CO_2 concentration during Cretaceous times. *Nature* 399 (6734), 342–345. doi: 10.1038/20659

Larkum, A. D., Drew, E., and Ralph, P. (2006a). "Photosynthesis and metabolism in seagrasses at the cellular level," in *Seagrasses: Biology, ecologyand conservation* (Dordrecht: Springer Netherlands), 323–345. doi: 10.1007/978-1-4020-2983-7_14

A. W. D. Larkum, R. J. Orth and C. M. Duarte (Eds.) (2006b). *Seagrasses : biology, ecology, and conservation* (Dordrecht: Springer).

Lewis, E. (1980). The practical salinity scale 1978 and its antecedents. *IEEE J. Oceanic Eng.* 5 (1), 3–8. doi: 10.1109/JOE.1980.1145448

Lewis, E., Wallace, D. W. R., and Allison, L. J. (1998). *Program developed for CO2 system calculations, carbon dioxide information analysis center*. Oak Ridge, Tenn: Oak Ridge National Laboratory.

Madsen, T. V., Maberly, S. C., and Bowes, G. (1996). Photosynthetic acclimation of submersed angiosperms to CO_2 and HCO_3^-. *Aquat. Bot.* 53 (1-2), 15–30. doi: 10.1016/0304-3770(95)01009-2

Madsen, T. V., and Sand-Jensen, K. (1991). Photosynthetic carbon assimilation in aquatic macrophytes. *Aquat. Bot.* 41 (1-3), 5–40. doi: 10.1016/0304-3770(91)90037-6

Madsen, T. V., Sand-Jensen, K., and Beer, S. (1993). Comparison of photosynthetic performance and carboxylation capacity in a range of aquatic macrophytes of different growth forms. *Aquat. Bot.* 44 (4), 373–384. doi: 10.1016/0304-3770(93)90078-B

McPherson, M. L., Zimmerman, R. C., and Hill, V. J. (2015). Predicting carbon isotope discrimination in eelgrass (*Zostera marina* l.) from the environmental parameters–light, flow, and [DIC]. *Limnology Oceanography* 60 (6), 1875–1889. doi: 10.1002/lno.10142

Meyer, M. T., Whittaker, C., and Griffiths, H. (2017). The algal pyrenoid: key unanswered questions. *J. Exp. Bot.* 68 (14), 3739–3749. doi: 10.1093/jxb/erx178

Miyake, C. (2010). Alternative electron flows (Water–water cycle and cyclic electron flow around PSI) in photosynthesis: Molecular mechanisms and physiological functions. *Plant Cell Physiol.* 51 (12), 1951–1963. doi: 10.1093/pcp/pcq173

Motulsky, H., and Christopoulos, A. (2004). *Fitting models to biological data using linear and nonlinear regression : a practical guide to curve fitting* (Oxford: Oxford University Press).

Munekage, Y., Hashimoto, M., Miyake, C., Tomizawa, K.-I., Endo, T., Tasaka, M., et al. (2004). Cyclic electron flow around photosystem I is essential for photosynthesis. *Nature* 429 (6991), 579–582. doi: 10.1038/nature02598

Osmond, C. B. (1981). Photorespiration and photoinhibition : Some implications for the energetics of photosynthesis. *Biochim. Biophys. Acta (BBA) - Rev. Bioenergetics* 639 (2), 77–98. doi: 10.1016/0304-4173(81)90006-9

Osmond, B., Badger, M., Maxwell, K., Björkman, O., and Leegood, R. (1997). Too many photons: photorespiration, photoinhibition and photooxidation. *Trends Plant Sci.* 2 (4), 119–121. doi: 10.1016/s1360-1385(97)80981-8

Ow, Y. X., Collier, C. J., and Uthicke, S. (2015). Responses of three tropical seagrass species to CO_2 enrichment. *Mar. Biol.* 162 (5), 1005–1017. doi: 10.1007/s00227-015-2644-6

Palacios, S., and Zimmerman, R. (2007). Response of eelgrass *Zostera marina* to CO_2 enrichment: possible impacts of climate change and potential for remediation of coastal habitats. *Mar. Ecol. Prog. Ser.* 344, 1–13. doi: 10.3354/meps07084

Pfannschmidt, T., and Yang, C. (2012). The hidden function of photosynthesis: a sensing system for environmental conditions that regulates plant acclimation responses. *Protoplasma* 249 (2), 125–136. doi: 10.1007/s00709-012-0398-2

Raghavendra, A. S. (2000). *Photosynthesis: A comprehensive treatise* (Cambridge, UK: Cambridge University Press).

Ralph, P. J., Durako, M. J., Enríquez, S., Collier, C. J., and Doblin, M. A. (2007). Impact of light limitation on seagrasses. *J. Exp. Mar. Biol. Ecol.* 350 (1-2), 176–193. doi: 10.1016/j.jembe.2007.06.017

Ralph, P. J., and Gademann, R. (2005). Rapid light curves: A powerful tool to assess photosynthetic activity. *Aquat. Bot.* 82 (3), 222–237. doi: 10.1016/j.aquabot.2005.02.006

Ralph, P. J., Polk, S. M., Moore, K. A., Orth, R. J., and Smith, W. O. (2002). Operation of the xanthophyll cycle in the seagrass *Zostera marina* in response to variable irradiance. *J. Exp. Mar. Biol. Ecol.* 271 (2), 189–207. doi: 10.1016/s0022-0981(02)00047-3

Rasmusson, L., Buapet, P., George, R., Gullström, M., Gunnarsson, P., and Björk, M. (2020). Effects of temperature and hypoxia on respiration, photorespiration, and photosynthesis of seagrass leaves from contrasting temperature regimes. *ICES J. Mar. Science.* 2056–2065. doi: 10.1093/icesjms/fsaa093

Raven, J., and Beardall, J. (2003). "Carbon acquisition mechanisms of algae: Carbon dioxide diffusion and carbon dioxide concentrating mechanisms," in *Photosynthesis in algae*. Eds. A. D. Larkum, S. Douglas and J. Raven (Dordrecht: Springer Netherlands), 225–244. doi: 10.1007/978-94-007-1038-2_11

Raven, J. A., and Beardall, J. (2014). CO_2 concentrating mechanisms and environmental change. *Aquat. Bot.* 118 (0), 24–37. doi: 10.1016/j.aquabot.2014.05.008

Raven, J. A., Giordano, M., Beardall, J., and Maberly, S. C. (2011). Algal and aquatic plant carbon concentrating mechanisms in relation to environmental change. *Photosynth Res.* 109 (1-3), 281–296. doi: 10.1007/s11120-011-9632-6

Ruesink, J. L., Yang, S., and Trimble, A. C. (2015). Variability in carbon availability and eelgrass (*Zostera marina*) biometrics along an estuarine gradient in willapa bay, WA, USA. *Estuaries Coasts* 38 (6), 1908–1917. doi: 10.1007/s12237-014-9933-z

Scheibe, R., Backhausen, J. E., Emmerlich, V., and Holtgrefe, S. (2005). Strategies to maintain redox homeostasis during photosynthesis under changing conditions. *J. Exp. Bot.* 56 (416), 1481–1489. doi: 10.1093/jxb/eri181

Schubert, N., Freitas, C., Silva, A., Costa, M. M., Barrote, I., Horta, P. A., et al. (2018). Photoacclimation strategies in northeastern Atlantic seagrasses: Integrating responses across plant organizational levels. *Sci. Rep.* 8 (1), 14825. doi: 10.1038/s41598-018-33259-4

Somerville, C. R. (2001). An early arabidopsis demonstration. resolving a few issues concerning photorespiration. *Plant Physiol.* 125 (1), 20–24. doi: 10.2307/4279600

Spreitzer, R. J., and Salvucci, M. E. (2002). RUBISCO: Structure, regulatory interactions, and possibilities for a better enzyme. *Annu. Rev. Plant Biol.* 53 (1), 449–475. doi: 10.1146/annurev.arplant.53.100301.135233

Tcherkez, G. G. B., Farquhar, G. D., and Andrews, T. J. (2006). Despite slow catalysis and confused substrate specificity, all ribulose bisphosphate carboxylases may be nearly perfectly optimized. *Proc. Natl. Acad. Sci.* 103 (19), 7246–7251. doi: 10.1073/pnas.0600605103

Tolbert, N. E., and Osmond, C. B. (1976). *Photorespiration in marine plants* (Baltimore: CSIRO).

Touchette, B. W., and Burkholder, J. M. (2000). Overview of the physiological ecology of carbon metabolism in seagrasses. *J. Exp. Mar. Biol. Ecol.* 250 (1-2), 169–205. doi: 10.1016/s0022-0981(00)00196-9

Voss, I., Sunil, B., Scheibe, R., and Raghavendra, A. S. (2013). Emerging concept for the role of photorespiration as an important part of abiotic stress response. *Plant Biol.* 15 (4), 713–722. doi: 10.1111/j.1438-8677.2012.00710.x

Webb, W., Newton, M., and Starr, D. (1974). Carbon dioxide exchange of *Alnus rubra* a mathematical model. *Oecologia* 17 (4), 281–291. doi: 10.1007/BF00345747

Xin, C.-P., Tholen, D., Devloo, V., and Zhu, X.-G. (2015). The benefits of photorespiratory bypasses: How can they work? *Plant Physiol.* 167 (2), 574–585. doi: 10.1104/pp.114.248013

Zeebe, R. E. (2012). History of seawater carbonate chemistry, atmospheric CO_2, and ocean acidification. *Annu. Rev. Earth Planetary Sci.* 40 (1), 141–165. doi: 10.1146/annurev-earth-042711-105521

Zimmerman, R. C. (2003). A biooptical model of irradiance distribution and photosynthesis in seagrass canopies. *Limnology Oceanography* 48 (1), 568–585. doi: 10.4319/lo.2003.48.1_part_2.0568

Zimmerman, R. C. (2006). "Light and photosynthesis in seagrass meadows," in seagrasses: Biology, ecology and conservation,". Eds. A. W. D. Larkum, R. J. Orth and C. M. Duarte (Dordrecht: Springer Netherlands), 303–321.

Zimmerman, R. C. (2021). Scaling up: Predicting the impacts of climate change on seagrass ecosystems. *Estuaries Coasts* 44 (2), 558–576. doi: 10.1007/s12237-020-00837-7

Zimmerman, R. C., Cabello-Pasini, A., and Alberte, R. S. (1994). Modeling daily production of aquatic macrophytes from irradiance measurements: a comparative analysis. *Mar. Ecol. Prog. Ser.* 114, 185–196. doi: 10.3354/meps114185

Zimmerman, R. C., Hill, V. J., and Gallegos, C. L. (2015). Predicting effects of ocean warming, acidification, and water quality on Chesapeake region eelgrass. *Limnology Oceanography* 60 (5), 1781–1804. doi: 10.1002/lno.10139

Zimmerman, R. C., Hill, V. J., Jinuntuya, M., Celebi, B., Ruble, D., Smith, M., et al. (2017). Experimental impacts of climate warming and ocean carbonation on eelgrass *Zostera marina*. *Mar. Ecol. Prog. Ser.* 566, 1–15. doi: 10.3354/meps12051

Zimmerman, R. C., Kohrs, D. G., Steller, D. L., and Alberte, R. S. (1997). Impacts of CO_2 enrichment on productivity and light requirements of eelgrass. *Plant Physiol.* 115 (2), 599–607. doi: 10.1104/pp.115.2.599

Zimmerman, R. C., Reguzzoni, J. L., and Alberte, R. S. (1995). Eelgrass (*Zostera marina* l.) transplants in San Francisco bay: Role of light availability on metabolism, growth and survival. *Aquat. Bot.* 51 (1-2), 67–86. doi: 10.1016/0304-3770(95)00472-c

Zimmerman, R. C., Reguzzoni, J. L., Wyllie-Echeverria, S., Josselyn, M., and Alberte, R. S. (1991). Assessment of environmental suitability for growth of *Zostera marina* l. (eelgrass) in San Francisco bay. *Aquat. Bot.* 39 (3-4), 353–366. doi: 10.1016/0304-3770(91)90009-t

Zimmerman, R. C., SooHoo, J. B., Kremer, J. N., and D'Argenio, D. Z. (1987). Evaluation of variance approximation techniques for non-linear photosynthesis–irradiance models. *Mar. Biol.* 95 (2), 209–215. doi: 10.1007/BF00409007